NATIONAL GALLERY OF ART

FINAL REPORT
TO THE
NATIONAL CENTER FOR PRESERVATION TECHNOLOGY AND TRAINING
1997 GRANT PROGRAM

1. Project type: Environmental Effects of Outdoor Pollutants on Cultural Resources

2. Project title: RESEARCH INTO PROTECTIVE COATING SYSTEMS FOR OUTDOOR BRONZE SCULPTURE AND ORNAMENTATION. PHASE II.

3. Recipient: : National Gallery of Art
Washington, DC 20565

Principal project contact: Dr. E. René de la Rie, Head, Scientific Research
(tel) 202-842-6669
(fax) 202-842-6886
(e-mail) rdelarie@csi.com

Principal investigator: Lynn B. Brostoff, Conservation Scientist
(tel) 412-268-4414
(fax) 412-268-3101
(e-mail) lynn2@andrew.crnu.edu

Research assistant: Tara Shedlosky
(tel) 202-789-4636
(fax) 202-842-6886
(e-mail) t-shedlosky(@nga.gov

4. Table of Contents: Page

Executive Summary

One hundred twenty two new samples, making up Phase II, were prepared for study. The samples consist of three sets of coated and uncoated substrates. The substrates are: I) satin-finish, cast monumental bronze, II) artificially patinated, cast monumental bronze, III) naturally patinated 50-year-old copper roof, and IV) pressure-blasted, naturally patinated 50-year-old copper roof The coatings are 1) Incralac+ wax, 2) benzotriazole (BTA) pretreatment+ wax, 3) Nikolas 11565 acrylic+ Nikolas 9778 acrylic urethane+ wax, 4) BTA pretreatrnent+ BASF 923-85 acrylic urethane+ wax, and 5) Nikolas waterborne acrylic urethane+ wax. Additional samples on rolled bronze, glass slides, and mirrored slides were also prepared. Sample set A consists of unweathered controls. Sample set B, in triplicate, was exposed to an accelerated weathering program. Sample set C is currently undergoing natural outdoor weathering on the roof of the National Gallery of Art. One sample substrate in each set is uncoated.

Activity during this grant period also included continuing evaluation of coating performance on Phase I samples,’ particularly those samples weathered outdoors. After 1.5 years on the roof of the National Gallery of Art, most coated samples were still holding up well, and in most cases accelerated weathering results appeared to be reasonably predicting performance under real conditions. Results from accelerated weathering of Phase Ti samples are compared to results of Phase I testing.

Introduction

This research addresses the continuing need for new coating strategies to protect outdoor bronzes from the effects of polluted environments. The goal of the present research is to form general hypotheses concerning how protective organic coatings work and fail on bronze surfaces when exposed to typical polluted, urban environments, and to make recommendations concerning coating practice in outdoor sculpture conservation. To this end, the research focuses on how coating performance may vary on different substrates and with different surface preparation. In Phase II of the research, reported here, we tested five common or new coating systems chosen from the 29 coatings tested in Phase I on polished, cast bronze and 50-year-old copper roof substrates. The five coatings in Phase II have been applied to an expanded range of typical copper alloy substrates and subjected to either a) no weathering, b) accelerated weathering, or c) natural outdoor weathering. The automotive-type, cyclic accelerated weathering regimen used in Phase II was harsher than in Phase I in order to increase the acceleration factor. Coatings used in Phase I and Phase II are listed in Table I for reference throughout the report. Photographs of Phase I, sets B and C samples (after accelerated and outdoor weathering), as well as Phase II samples before, and, for set B, after weathering, are attached to the report.

Sample analysis methodology in Phase 1.1 is basically unchanged from Phase 1, and includes various visual methods of coating performance assessment, as well as infrared reflectance spectroscopic techniques for analysis of the chemistry at the metal/coating interfaces. Preliminary overall failure ratings were obtained for Phase II samples after accelerated weathering by an improved system, which was then used to re-evaluate Phase I samples for better consistency.

Experimental Methods

Accelerated weathering of sample set B consisted of an automotive-type, accelerated weathering program, modified from ASTM standard test procedures and SAE standards[2] for an Atlas Ci65a xenon-arc Weather-ometer and a Tenney Thirty temperature/humidity test chamber. Total accelerated weathering time was 120 days. This testing regimen consisted of two types of exposure: 1) constant light and intermittent back- or specimen-spraying in the Weather-ometer, and 2) alternating humidity cycling and freeze-thaw cycling in the Tenney, including daily, manual spraying during the weekdays with a concentrated “rain” solution. For the first 27 days samples were alternated between Tenney and Weather-ometer exposures, and the spray solution average ion concentration was, in meq/l: $[SO_4^=]=12.16$; $[NO_3^-]=4.8l$ $\{NH_4^+\}=l4.65$, $[CI^-]=34.38$; $[Na^+]=34.34$. The pH of this solution was 4.2. The subsequent 37 days of weathering were Weather-ometer exposure only, with deionized water spraying. Average conditions in the Weather-ometer, using a borosilicate/borosilicate inner and outer glass filter combination, were:
black panel 60.5 °C, relative humidity 23-44 %, irradiance 0.55 W/m^2 @ 340 nm. The final 56 days of weathering were Tenney exposure only. The medium chloride rain solution used here was formulated to represent approximately 100x the maximum concentration of common ions reported for typical acid rain,[3] but with a lower chloride content than normally used in accelerated weathering studies.[4] Total average ion concentration was, in meq/l: $[SO_4^=]=15.30$; $[NO_3^-]=4.80$; $[NH_4^+]=4.18$; $[C_1^-]=22.07$; $[Na^+]=35.37$, The average pH of this solution was 3.64. In order to increase “time of wetness” following rain solution spraying in the Tenney, conditions were held at 23 °C and 80% RH for a period of one to three hours. Otherwise, conditions in the Tenney were cycled between 20 and 85 % RH, or between (-15) °C and 60 °C, in four hour segments. Samples were thoroughly rinsed with room temperature supermillipore water after weathering and conditioned to room temperature and humidity.

The Phase II substrates were examined by scanning electron microscopy (SEM) and energy dispersive spectroscopy (EDS). SEM/EDS was performed using a JEOL 6300 scanning electron microscope equipped with a Link Super ATW Si(Li) detector and a Link eXL II spectrometer. The accelerating voltage was 10-20 kV, depending on the sample. Metal substrates were analyzed by secondary emission energy dispersive X-ray fluorescence spectroscopy (XRF) using a Kevex 0750A spectrometer equipped with a BaCI2 secondary target and 6 mm collimators. The anode voltage and current were 60 kV and 0.4 mA, respectively. Live accumulation time was 200 seconds. Elemental weight percentages were calculated with EXACT (energy dispersive X-ray analysis computation technique), a software program provided by Kevex.

Selected corrosion products and patinas were analyzed by powder X-ray diffraction (XRD) using a Philips X-ray generator 3 100 equipped with a copper target and nickel filter to provide Cu Ka radiation, 45 kV anode voltage, and 25 mA current. Additional open architecture XRD analysis was run by Dr. George Wheeler, the Metropolitan Museum of Art, NY, NY, on a Philips 1710 open-architecture diffractometer with Cu Kα radiation acquired at 30 mA, 40 kV, 0.02 °/sec. In the latter system, peaks were recorded and marked from the 1710 by Sietronic Software and transferred to the Fein-Marquart software program.

Coatings on the samples were characterized under low magnification for overall film quality in terms of the presence of seeds, orange peel, air entrapment, solvent popping, hazing or whitening, bumps and sinks, cratering, and crawling/dewetting, according to common industrial definitions.[5] Dry film thickness and its standard deviation (ASTM D1400) on sample sets A and

B after weathering were determined using an Elcometer 345 dry film thickness gauge. Ten to twenty readings were taken on each sample. The bronze coating measurements were subject to an error of ± 0.1 mil (2.5 microns), and thus coatings or patinas less than about 0.2 mils could not be measured accurately. The copper roof samples had a large margin of error, which could not be determined due to the extremely rough and uneven patina. Sample sets A and B were also evaluated for coating adhesion by the ASTM D3359 cross-cut or X-cut adhesion tape test. It was observed that adhesion ratings were affected by coating thickness and apparent cohesive strength. This is discussed more frilly in “Results and Discussion.”

Coating characterization before and after weathering involved various techniques of Fourier-transform infrared spectroscopy (FTIR). All FTIR spectra were collected in absorbance with a Bio-rad FTS-60A equipped with a UIMA300A microscope. Bulk coating analysis was performed by microtransmission using a diamond cell, or by specular reflectance from aluminized mirrors using a Harrick fixed angle specular attachment. Attenuated total reflection (ATR) spectroscopy of selected coatings delaminated from the metal substrates by immersion in liquid nitrogen, or simply peeled off when possible after accelerated weathering, was performed with a Harrick 4x beam condenser fitted with a delrin holder for SPP crystals with faces measuring 10 x 5 x 1 mm. The IRE crystals used in this study were KRS-5 45°, KRS-5 60°, and Ge 45°. Calculated depths of penetration for these crystals were, respectively, 2.92, 1.56, and 1.53 micrometers.[6] For samples, which were smaller than the crystals, multiple samples were placed together on the holder and exposed areas were masked with aluminum foil. ATR spectra were corrected for wavelength dependency using the “atrcorr.ab” function in the Grams 32/Win-JR software. Reflection-absorption infrared (RAIR) spectroscopy was performed on thin films of some coatings or pretreatments on reflective bronze or copper using a Harrick versatile reflection attachment for center-focused beam fitted with a retro-mirror accessory and a wire-grid polarizer set for parallel beam polarization. The angle of incidence was 78 or 85 degrees. All CuBTA films on rolled bronze were examined at 78 degrees.

Coatings were analyzed by pyrolysis-gas chromatography/mass spectrometry (Py-GC/MS) using a CDS 2000 Pyroprobe mounted directly onto the injector of a Varian 3500 capillary gas chromatograph equipped with a RTX-1 column (32mm ID, 30 m, .25 microns film thickness) and interfaced to a Finnigan 800 Ion Trap Detector (ITD). Pyrolysis was carried out at 600 °C for 10 sec; the Py-GC interface was held at 300 °C; the GC oven was programmed with an initial temperature of 40 °C (held for 5 mm.) and increased to 300°C (held for 10 mm.) at a rate of 8 °C/min. The column was interfaced directly to the ITD; the transfer line was at 250°C. The scan range was 35-550 amu, scan time 1 sec., and data analysis was with Finnigan ITD 4.10. The split/splitless injector was at 300 °C in the split mode, with a split ration of about 100:1; the carrier gas was helium.

Coating performance was evaluated in terms of failure for Phase I, sets IB, IC and IIB (polished bronze after accelerated and natural weathering, copper roof after accelerated weathering) based on ratings in the following categories: a) texture change (including surface spotting/etching), b) flaking/peeling, c) hazing or whitening, d) blister/cracking/checking (ASTM D714, D660), e) color change, f) overall corrosion, and g) corrosion at the scribemark. Ratings were given on a scale from 0-5, where: 0=not present; l=barely noticeable; 2=slightly noticeable; 3=noticeable; 4=very noticeable; 5=dramatic. Category “f” included overall pitting corrosion, rated according to ASTM D610, normalized to a 0-5 scale, and augmented for large areas of oxidation or other corrosion. For set IB samples, after 1200 hours accelerated weathering mean linear creepage of corrosion at a scribemark (ASTM 1654) was measured under 40x magnification approximately every 1/8” along each side of the scribemarks, and measurements (mm) were normalized to a 0-5 scale.

After rating appropriate groups of samples, “total failure ratings” were obtained according to the formula: (a + b + c + d + e) + (10f + 5g), where the sum (a:e) equals the coating performance contribution, and the weighted sum of (f + g) equals the total corrosion contribution. This formula was found to fit empirical ranking quite well. For ratings after 1200 hours accelerated weathering, coating failure appeared insignificant and was not included in the failure rating. The majority of Phase I, set IIC samples (copper roof, natural weathering) did not exhibit high degrees of failure in any category. Samples IIC were thus only grouped into rough categories of better and worse performance. Overall coating performance ratings for Phase II, sample set B have not been completed and are reported here both in empirical order of performance, and as preliminary total failure ratings derived from visual appearance in all the categories mentioned above.

Electrochemical impedance spectroscopy (EIS) was performed on five bronze samples from Phase I in the laboratory of Dr. Gordon Bierwagen, North Dakota State University, using a Gamry PC3 potentiostat controlled by Gamry CMS 100 software. A saturated Calomel electrode was used as the reference electrode with a platinum counter electrode. Measurements were taken between 0.1Hz to 5000 Hz with 10 millivolts RMS sine wave potential. Ten points were collected per decade. The area of exposure was 12.56 cm^2, using Dilute Harrison’s electrolyte (0.35wt% $(NH_4)_2)SO_4$, 0.05wt% NaC1).

Preparation and Description of Phase II Samples

SUBSTRATES

The 122 Phase II samples are 3” x 5” coated or uncoated metal coupons. Sixty two of the metal substrates are a “monumental” bronze alloy (analysis below), cast and finished by Bedi Makky Foundry in Brooklyn, NY. Thirty-two of these samples were water-polished at the foundry to a satin finish, and the remaining were wheel-polished to 120 grit, then artificially patinated to a warm, medium brown color. The patina was commissioned as a typical potassium sulfide/ferric nitrate patina, but was later reported to be produced by a one-step process with heat using a dilute solution of ferric nitrate in tap water with one or two drops of cupric nitrate and with no rinsing. However, XRD analysis of the patina suggested that patination included ammonium sulfide, as discussed below.

The remaining substrates are coupons of copper roofing, which have a natural, light green brochantite patina (analysis below) produced over about 50 years at about a 30 degree incline and southern exposure. Although the patina is fairly even, there are yellowish depressed spots and tiny, raised black dots on the surfaces. The roofing was recently removed from the Library of Congress in Washington, DC, and was generously donated by the Architect of the Capitol. Half of the copper roof samples were pressure-blasted with Agrashell ground English walnut shells, AD-10.5B mesh. The manufacturer reports that the shell oil content is 0.5% by weight. Cameron Wilson, outdoor sculpture conservator, carried out blasting using about 40 psi at a slight angle, roughly 8-10 inches from the surface. The color of the substrates after blasting is a much darker green overall, with yellowish spots and tiny black dots still remaining.

SUBSTRATE PREPARATION

All substrates underwent cleaning prior to coating. The polished, cast bronze substrates were immersed in a xylene bath, then wiped with xylene, then “Acryli-clean” using a soft, clean cloth. This was followed by an acetone bath, then alternating wipes with acetone, ethanol and Acryli-clean, until the substrate passed the water drop break test.[7] The artificially patinated bronze coupons received only brief acetone baths, followed by wiping with acetone and ethanol. Some loose brown patina was removed during this procedure. Unblasted, copper roof substrates were first bathed and lightly scrubbed in distilled water with a small amount of Triton-X surfactant added, then rinsed and air-dried. These substrates are referred to as water-washed copper roof throughout the report. Both blasted and unblasted, water-washed copper roof samples were additionally soaked for about 3 minutes in a xylene bath, then bathed briefly in acetone, followed by wiping with acetone and ethanol. Acryli-clean wax and grease remover DX330 is a commercial solvent from PPG, Inc. The other solvents were reagent grade.

COATINGS

Five coatings were applied to all but 20 substrates, which were retained as uncoated controls. One of each type of uncoated substrate in set B was treated with BTA (see “Coating Application”). One extra polished, cast bronze sample was coated with an experimental organosilane developed by Dr. W.J. van Ooij of the University of Cincinnati, and then waxed. The five coatings are as follows: 1) 2 coats Incralac + wax, 2) benzotriazole (BTA) pretreatment + wax, 3) Nikolas 11565 acrylic + Nikolas 9778 acrylic urethane + wax, 4) BTA pretreatment + 2 coats BASF 923-85 acrylic urethane + wax, and 5) 2 coats Nikolas waterborne acrylic urethane + wax. All waxing consisted of two brush coats followed by light buffing. One extra polished bronze sample was coated with Incralac and left unwaxed.

In 1964 the International Copper Research Association (INCRA) developed Incralac, a commonly used coating on outdoor bronzes. It is an unpatented formulation made from Acryloid B-44, a thermoplastic methyl methacrylate copolymer manufactured by Rohm and Haas; the corrosion inhibitor benzotriazole (BTA) (often referred to as a chelating agent); and a leveling agent, in this case a silicone oil. The sole manufacturer of Incralac in the United States at present is StanChem, Inc., in East Berlin, CT. Their literature states that Incralac is formulated from “a blend of acrylic resins,” and also contains “a U.V. absorber and a chelating agent.” This manufacturer claims that they are producing Incralac according to the original formulation.

Nicolas Veloz, outdoor sculpture conservator, supplied the wax coating. It is a blend of about 75% Bareco Victory Wax (microcrystalline, synthetic, low melting point wax), plus Bareco Polywax 2000 and 500 (polyethylene microcrystalline waxes), and Petronauba C, an oxidized polyethylene wax. This coating has no BTA.

The Nikolas 11565 Outdoor Lacquer is a “modified acrylic” lacquer designed for exterior brass and bronze, and is supplied ready for use. The manufacturer reports that this coating contains BTA as a “chelating agent,” as well as UV absorbers. In addition, the literature states that, “[b]ecause of its excellent flowing capabilities, orange peel is virtually eliminated” at thinner coatings.[8] Nikolas 9778 Exterior Uralac is a room temperature cure, two-component urethane developed for exterior lighting, exterior hardware, automotive trim, exterior signage, and sporting goods, including gold-plated, brass, and silver-plated metals. it is based on a hydroxylated acrylic polyol, reacted with an aliphatic polyisocyanate to form urethane crosslinks. Side products are typically also formed in these systems, including amines, disubstituted ureas and substituted biurets, and allophonates.[9] Catalysts, flow aids such as silicones, UV absorbers, including BTA, and defoamers are typically added to these coatings. The manufacturer confirmed that this coating contains BTA and other UV absorbers.

BASF Glassodur-MS Top Clear 923-85 is a two-component, high solid acrylic urethane formulated from a proprietary acrylic copolymer crosslinked with a trimer of hexarnethylenediisocyanate (HDI). The manufacturer reports that this coating contains BTA. The coating was developed for the automotive refinishing industry, but has also seen limited application in the conservation of outdoor metal objects.

Nikolas 11560 Eco-borne Brass Lacquer is a one-component, waterborne acrylic urethane. Although designed for the interior metal maintenance market, it is also marketed for exterior applications. The manufacturer confirmed that the coating contains BTA, but no additional UV absorbers.[10]

COATING APPLICATION

BTA pretreatments consisted of several brush applications of 1 .5% (wt) BTA/ethanol solution, air-drying, and rinsing with ethanol. Incralac coatings were applied in a 60:40 reduction in xylene. On all of the patinated substrates Incralac was applied first with a brush coat, then with a spray coat. On the polished bronze, both coats of Incralac were spray-applied. All other lacquer coatings were spray-applied as per manufacturer recommendations as follows. The Nikolas acrylic was applied as one coat without reduction, and the Nikolas 9778 was mixed parts A:B in a ratio of 9:1, reduced 50% in special thinner, and applied in a single coat over the acrylic after 30 minutes. The BASF acrylic urethane was mixed parts A:B in a 2: 1 ratio, reduced 50%, and spray-applied after a final wipe on the substrates with the BASF reducer. The Nikolas 11560 was sprayed as a single coat after reducing 5% in water. Cameron Wilson, outdoor sculpture conservator, applied all these coatings; spray pressure was about 35 psi in all cases. A second coat of 11560, reduced 5% in distilled, deionized water, was brush-coated onto the last set of coated samples about one week later, and, after sufficient curing, all the samples were waxed with two coats of a wax. Andrew Baxter, outdoor sculpture conservator, applied these supplemental coatings.

Sample set A, the controls, is made up of one of each type of sample, totaling 24 samples. The 74 samples in set B are comprised of three of each type of sample; these were set up for accelerated weathering exposure. One extra polished bronze sample coated with lncralac was left unwaxed and grouped with the B’s, as was the silane-treated and wax-coated, polished bronze sample. The remaining single samples comprise sample set C, which were placed on wooden racks at a 45 degree angle, due south, on the roof of the National Gallery for natural outdoor weathering. Before weathering, sample sets B and C were scribed through the coatings on the bottom half of the sample with an “X.”

A small group of additional samples were prepared by draw-down coating application on solvent-cleaned, rolled bronze coupons. Because of the varying viscosity of test coatings, uniform thickness between coatings was difficult to achieve. Additional samples of coatings on glass slides and aluminized mirror slides were prepared for accelerated weathering, but removed after 46 days due to poor condition.

Results and Discussion

SUBSTRATE CHARACTERIZATION

SEM imaging of the Phase TI sample substrates shows that the polished, cast bronze surface (Figure la) contains a fair amount of scratches and pits. XRD open architecture analysis detected copper tin/copper zinc alloy phases and lead phase separately. This concurs with backscattering SEM image of the bronze, which showed the lead precipitated in small globs throughout a two-part matrix. XRD also identified the presence of two tin oxides.

SEM of the artificial patina on bronze samples (Figure 1b) reveals a patchy, finely cracked mineral layer. This fissuring is finer in some areas than in others. EDS analysis of the artificial patina showed the presence of iron spread unevenly across the surface. No chloride or potassium was detected. The presence of sulfur could not be determined due to overlap with metal peaks. Aluminum and silicon were also detected; these are common contaminants, most likely found in the foundry environment. The average thickness of the patina was 0.2 mils (5 microns), which is less than experimental error using this method of measurement.

XRD open architecture analysis of the artificial patina, sampled by scraping off the metal, yielded a clear pattern which could be reasonably identified through the international JCPDS files with only two phases: ammonium iron sulfate [$(NH_4)_3Fe(SO_4)_3$] and copper nitrate hydroxide [$Cu_2(OH)_3NO_3$]. These two substances account well for most, but not all the peaks found in this sample. No iron oxides could be convincingly matched, although this does not rule out their presence in minor quantities, especially in poorly crystallized forms. These identifications imply that ammonium sulfide, a common patinizing agent, was in fact used in the patination, possibly present as a contaminant in the solution or the brush.

XRF analysis of the copper sheet indicated that the copper has a purity of 99.93%. XRD analysis of the patina, both by powder diffraction and open architecture, provided positive identification of the following crystalline phases: copper, cuprite (Cu_2O), brochantite-O (orthorhombic and monoclinic mixture) ($Cu_4\ SO_4(OH)_6$), antlerite (minor; ($Cu_3\ SO_4(OH)_4$)), and possibly copper sulfide. No tenorite (CuO) or copper chlorides were detected by these methods. The black spots were shown to have an identical pattern to the general green patina, containing only cuprite, brochantite, and possibly copper sulfide, with only one new but faint line at d=3.32 A, which could not be identified. The Fourier-transform infrared (FTIR) spectrum of the patina showed excellent agreement with the spectrum of pure brochantite,[11] No differences between the green and black patina components were detected by FTIR.

As described in the “Final Report to the NCPTT 1996 Grant Program,” SEM imaging of the copper roof patina (Figure 2a) shows a very rough, but finely textured and porous morphology. EDS analysis of the green patina revealed the presence of aluminum, silicon, iron, and phosphorous contaminants in addition to copper, sulfur, and oxygen. The presence of phosphorous in outdoor bronze and copper patinas has been sporadically noted, particularly in connection with black spots on copper patinas, and has been variously attributed to airborne fertilizer-containing particles or pigeon droppings.’2 The other contaminants are commonly found in airborne dirt particles. No carbon was detected. (Nitrogen cannot be detected from this detector array.) It is interesting that SEM/EDS analysis of black spots in the patina revealed the presence of chlorine, calcium, and vanadium, the latter for which we can offer no explanation. The presence of silicon as well as aluminum also appeared relatively higher in this spot.

SEM of the walnut shell-blasted copper roof, shown at half the magnification of the unblasted roof surface (Figure 2b) shows a surface in which the voids in the top mineral layer appear greatly exaggerated. The mineral layer also appears denser and more compact or matted down, with fine cracking visible in spots. EDS results for blasted copper roof coupons, both with and without subsequent solvent cleaning, matched those for the unblasted surface with the notable exception of a carbon peak in both spectra. This evidence appears to confirm suspicions that walnut shell blasting leaves oily deposits which are not easily removed from the surface of treated metals. FTIR of the blasted patina was ambiguous regarding the presence of oil, however.

Surprisingly, we could not detect any measurable difference in the average patina thickness on substrates with or without walnut shell blasting using the Elcometer gauge. For both types of copper roof substrates the average patina thickness reading was 0.70 mils ± 0.1. However, open architecture XRD analysis of the patinas on the respective substrates detected not only brochantite, but a substantial amount of copper and cuprite in the case of the blasted copper roof This implies that the patina was somewhat thinner on the blasted surface, enabling the X-rays to penetrate more deeply into the metal.

CORROSION ANALYSIS AFTER ACCELERATED WEATHERING

Table II contains a descriptive summary of corrosion on the weathered samples. XRD powder diffraction analysis of brown, black and green corrosion which formed on uncoated, polished cast bronze samples after 21 days of accelerated weathering showed that the primary phases being formed were red cuprite, green copper hydroxy sulfates (including brochantite-O and possibly posnjakite), nantokite, green to black copper hydroxy chlorides, and what may tentatively be identified with various zinc sulfate hydrates and/or copper zinc sulfates. Copper sulfides, which are mostly black or brown, do not crystallize well and are difficult to identify, and thus should not be ruled out. FT1.R of the corrosion product confirmed the presence of sulfates and nitrates. The FTIR spectrum also showed that copper hydroxy chlorides include atacamite as the major phase. It should be noted that in all cases of chloride identification, the presence of paratacamite and zincian paratacamite cannot be ruled out.

XRD open architecture analysis of the black and green corrosion, which formed on uncoated, polished bronze after completion of accelerated weathering, showed some differences. Identifiable phases include: cuprite (red); tenorite (black); and chlorides, including atacamite/paratacamites and botallackite (green/black), and what may reasonably be identified as zinc chloride sulfate hydroxide hydrate (white). No copper hydroxy sulfates were matched from these analyses, although an unassigned peak near 6.54 Å in patterns obtained after weathering may be related to an unidentified form of copper sulfate. The uncoated, polished bronze treated with BTA appeared very slightly less corroded after accelerated weathering, notably in terms of black corrosion. XRD of this substrate, however, yielded almost identical results, but with an additional peak at 3.220 Å attributable to stannic oxide, suggesting that somewhat less of the same phases occurred during weathering on the BTA-treated substrate.

Analysis of the patinated bronze after accelerated weathering showed that the patina had changed dramatically in terms of chemical makeup as well as color, having largely turned a gray-black color with a purplish reflection and light green spots; the original brown remained at edges only. Neither the original copper nitrate hydroxide, nor the ammonium iron sulfate was in fact detectable by open architecture XRD. The pattern obtained for this substrate showed a good match with those formed on unpolished bronze, with the exception of a new peak near 4.3 Å and the absence of tenorite. The metallic character of the black color suggested the presence of a sulfide, although sulfides could not be identified nor confirmed. The uncoated, patinated sample treated with BTA appeared somewhat less corroded, with more brown remaining. XRD analysis of this substrate confirmed the continued presence of the cupric nitrate product contained in the patina, but also revealed new, unassigned peaks near 12.6 and 4.4 Å, as well as the absence of tenorite and botallackite.

Open architecture XRD analysis of the black and green corrosion on the uncoated copper roof patina after accelerated weathering showed several new peaks and changes in peak intensities. These were identified with the formation of new cuprite and new brochantite (visible as darker green toward the bottom of the samples), plus a new product, tentatively identified as ammonium copper chloride hydrate. The latter product was not detected, however, on the BTA-treated coupon, which also appeared less corroded in terms of the absence of black products.

Analysis of the uncoated, blasted copper roof coupons, which weathered differently than the unblasted substrates, showed a new peak identifiable with paratacamite, along with evidence of new cuprite and brochantite formation. On the BTA-treated substrate, however, the chloride was not detected. Intensity changes and slight peak shifts detected in corrosion from the BTA-treated substrate did suggest that new cuprite and copper hydroxy sulfate were formed, though. These results indicate that blasting of the substrate made it more susceptible to corrosion, but that this could be slowed by BTA treatment.

In general, corrosion products detected after accelerated weathering were expected, supporting the accelerated weathering methodology used here as reasonable. One exception, however, was the tentative identification of an ammonium salt found on the copper roof, a substrate which tends to most effectively hold water/salts and may be more sensitive to higher concentrations of ammonium ions in the artificial rain solution than are found naturally. Results also generally point out that the artificial patina made for this study, as well as the blasting of the natural brochantite patina, caused substrates to be comparatively less stable to corrosion. This is reflected in the order assumed by the four substrates in the graph of failure ratings, Figure 14.

INTERFACIAL CHEMICAL ANALYSIS AFTER WEATHERING, PHASE I

FTIR and ATR were used to investigate the bulk vs. the polymer/metal interface of several coating systems, including Incralac and the 9778 acrylic urethane, from Phase I. These results are reported in the “Interim Report to the NCPTT 1997 Grant Program,” and in: Lynn B. Brostoff and B. René de la Rie, “Chemical Characterization of Metal/Coating Interfaces from Model Samples for Outdoor Bronzes by Reflection-Absorption Infrared Spectroscopy (ATR) and Attenuated Total Reflection Spectroscopy (ATR),” Proceedings, Metal 98, An international Conference on Metals Conservation, ICOM CC Metals Working Group, May 26-29, 1998, Draguignan, France, 320-328.

In summary, RAIR and ATR were used to investigate three coating systems before and after accelerated weathering: Incralac, StanChem waterborne acrylic urethane, and Nikolas 9778 solvent-borne acrylic urethane. Chemical information about the polymer interfaces against glass, rolled copper, patinated copper, and/or bronze, gathered by these methods, before and after accelerated weathering, was compared to FTIR microtransmission spectra of the bulk polymers.

Results revealed the existence of some chemical differences in the interfacial regions vs. the bulk coatings. In particular, only weak interactions between Incralac and copper or bronze substrates were detected, supporting ratings we obtained of mediocre adhesion. ATR of the

Incralac/copper interface also showed evidence for the development of long-range order or semi-crystallinity at surfaces, as well as polymer degradation at the metal interface, but not in the bulk,
after accelerated weathering of a thin coating.

Spectroscopic analysis of the waterborne acrylic urethane showed the persistence of some reactive species in the bulk polymer after curing, and even more numerous reactive species near the metal interface, including unreacted isocyanate. ATR spectra after weathering provided clear evidence of accelerated degradation reactions at both the bronze and, in particular, the copper mineral interfaces.

Bulk and ATR spectra of the solvent-borne acrylic urethane showed some interesting differences between the polymer cured on glass and on bronze, as well as some differences in composition at the metal interface vs. the bulk. Despite the fact that IR methods showed only very minor change in the polymer after weathering, increased relative concentrations of moisture-reactive species were detected at the polymer/bronze interface, indicating the coating system is sensitive to reactions with the bronze and is subject to degradation which will most likely show its effect with further weathering. In general, these results helped to elucidate comparative coating performance we observed after accelerated weathering. Furthermore, results appeared to predict performance problems that we have not yet seen in our weathering program.

RAIR and ATR analysis of Phase H samples will be performed during Phase III of this study.

COATING ANALYSIS

Bulk Chemical Analysis

As previously reported ("Final Report to the NCPTT 1996 Grant Program,"), py-GC/MS analysis of Incralac identified the major fraction as methyl methacrylate. Two smaller fractions were identified as ethyl acrylate and ethyl methacrylate, both of which were also identified in the raw B-44 resin. In addition, a very small fraction of butyl methacrylate, which was not found in the sample of B-44 analyzed here, was identified. Py-GC/MS also revealed the continued presence of solvent molecules in films of both B-44 and Incralac that were applied to glass, slides about one year prior to analysis. No stabilizers or UV absorbers, including BTA and Tinuvins 292 or 328, were detected in Incralac, or any of the other coatings, by this method. BTA is, however, known to be formulated in Incralac. RAIR of a rolled bronze coupon before and after coating with Incralac showed that, in fact, a very thin copper-BTA complex film remained on the surface of the metal after removal of Incralac by solvent immersion.

FTIR spectra of bulk Incralac suggested the presence of a small portion of carboxylic acid functionalities in the polymer, absorbing as a shoulder near 1700 cm^{-1} Methacrylic acid is commonly copolymerized with other polymers in order to slightly modify the end polymer in terms of carboxylic acid functional groups, and thus enhance adhesive properties. ATR spectra spectra of slightly weathered Incralac films on rolled copper, taken from both the air/polymer interface and copper/polymer interface, showed the presence of this shoulder on the air side, but its absence on the metal side. This suggests that carboxylic acid groups complex or otherwise bond to the metal surface.

Specular reflectance of Incralac films after weathering on an aluminized mirror showed a broad, weak absorption due to —OH groups. This appears to be related to a small amount of water uptake in the film during weathering.

The Veloz wax coating, as reported by the proprietor of this recipe, is a blend of about 75% Bareco Victory Wax (microcrystalline, synthetic, low melting point wax), plus Bareco Polywax 2000 and 500 (polyethylene microcrystalline waxes), and Petronauba C, an oxidized polyethylene wax. As previously mentioned, no BTA is added to this formulation. This information was consistent with the FTIR spectrum of the wax. No change in the wax on an aluminized mirror after 46 days accelerated weathering was detected by FTIR specular reflectance, although little of the wax remained on the mirror after this amount of time.

The FTIR spectrum of bulk Nikolas 11565 lacquer appeared to be a good match with Acryloid B-48, a copolymer with reportedly more flexibility than B-44 and better adhesion to metal surfaces,[13] and was thus assumed to be based on this or a similar resin. Py-GC/MS of this coating confirmed that the major fraction is methyl methacrylate, with additional fractions of butyl acrylate and butyl methacrylate. This again matched results for B-48.

The Nikolas 9778 Exterior Uralac acrylic urethane is an acrylic polyol/diisocyanate system. Py-GC/MS showed that the unmodified components of the uncrosslinked acrylic polyol (part A) consist of a copolymer of polystyrene, and methyl methacrylate, butyl acrylate, and n butyl methacrylate. The FTIR bulk microtransmission spectrum of the uncured acrylic polymer (part A) showed vibrations centered near 3520 and 1074 cm^{-1} which may be assigned to hydroxyl functionalities. The FTIR bulk microtransmission spectrum of a film cured on bronze showed intensification of the peak at 1725 cm^{-1}, indicating the presence of urethane crosslinks in the coating. However, new peaks absorbing near 3393, 1685 (shoulder), 1637 (weak), and 1519 cm^{-1} may be assigned mainly to NH vibrations and NCO urea vibrations. The urea(s) formed appear to match with the spectrum of the autocrosslinked diisocyanate, suggesting a fair amount of the crosslinking agent has both reacted with itself and formed urea linkages. (It is supplied as a trimer, but reacts readily with atmospheric moisture by itself) Furthermore, the continuing presence of absorption peaks near 3520 cm’ indicates that crosslinking did not take place at all active sites. The latter effect is the inevitable result of moisture contamination during application and curing of the coating.[14]

After accelerated weathering on bronze in Phase 1, the FTIR rnicrotransmission of the bulk coating showed signs of further curing in the greatly intensified and shifted carbonyl peak near 1731 cm-1 and in reduction of peaks attributed to hydroxyl groups. After accelerated weathering in Phase II, specular reflectance of the 9778 applied onto rolled bronze showed the disappearance of peaks near 1520 and 1636 cm^{-1} attributed to a urea linkage, as well as an increased shoulder near 1692 cm^{-1}. The latter effect could be related to the development of CC and/or C=N groups; this will be investigated in future work.

FTIR of the BASF 923-85 acrylic urethane after room temperature curing for l 1/2 months showed unreacted isocyanate species absorbing near 2260 cm^{-1} This film did, however, pass a solvent test for a cured film, i.e., was not marred by rubbing with a bit of the reducer. After heating @ 100 °C for 3 days, the isocyanate peak disappeared. Specular reflectance of a film applied to an aluminized mirror showed no isocyanate peak after 46 days of accelerated weathering. This method also revealed changes in the double COO/NCOO/NCON peaks at 1736/1688 cm^{-1} after weathering, indicating additional changes from curing.

FTIR analysis of the Nikolas 11560 waterborne acrylic urethane showed a relatively small proportion of phenyl vibrations and a relatively large proportion of NH/OH vibrations. Py GC/MS analyses showed main components of polymer resin are styrene, butyl methacrylate, and an alcohol. FTIR specular reflectance of a film on an aluminized mirror before and after accelerated weathering for 46 days did not show any detectable changes in the bulk film.

Coating Quality, Phase II

Coatings were examined for defects, including the presence of seeds (particulate contaminants), cratering, orange peel, solvent popping/air entrapment (commonly described as pinholing). These defects may affect aesthetic appearance as well as performance. An obvious example is pinholing, which often results in local corrosion pits. Thickness fluctuation also has important bearing on performance since it will set up differences in permeability and possibly in electrochemical potentials. Thickness variation occurs in orange peel on a micro-scale, and is also reflected on a larger scale in the standard deviation of the thickness readings for all the coatings. Normal spray application of coatings inevitably results in defects, and multiple layers of coatings, applied at right angles if possible, are usually recommended to offset many defects, although layers may exaggerate thickness variation. A thin wax topcoat may be quite beneficial in this respect. It is also known that residual stresses built up during film formation may be associated with adhesion loss and/or cracking and crazing.[15] it is interesting to speculate whether orange peel, which is caused by flow problems associated with high film viscosity or surface tension gradients during film formation, may also be associated with stress-related loss of adhesion or cohesion.

Incralac was observed to have medium orange peel on the bronze substrates, and a fine, bumpy appearance on the copper roof substrates, despite efforts to avoid these defects. The wax coatings were applied very thinly by brushing, followed with polishing, as is common practice. They generally looked good, achieving a matting effect, as desired, on top of the shiny coatings. After waxing, the blasted copper roof substrate was particularly saturated in appearance, achieving a matte, fairly brown coloration. The Nikolas acrylic/acrylic urethane coating showed light orange peel on the cast bronze substrates, although this was largely masked by waxing. Much practice and experimentation were necessary to avoid orange peel in the BASF acrylic urethane coatings, and, as reported above, a 50% reduced coating was finally used for this purpose and was generally successful. A small amount of air entrapment was noted on the patinated bronzesubstrates, and seeding substrates. However, seeding was a large problem here. Compared to the other substrates, this coating also produced a darker green appearance on the unblasted copper roof. The Nikolas waterborne acrylic urethane exhibited severe solvent popping and/or air entrapment, visible mostly on the polished bronze and unblasted copper roof substrates, despite following the manufacturer's recommendations for ways to avoid this. Cratering and seeding were also visible in this coating.

In a few cases, coatings were found to show some changes after 8 months of exposure only to either normal room conditions (controlled museum conditions) or storage in a Tenney controlled environmental room. The wax coatings showed some bloom, i.e., small opaque patches under magnification. The uncoated, artificial patina had also noticeably changed, appearing darker and somewhat patchy. This change is not unexpected, according to common observation, especially for patinas formed with sulfide compounds. However, the chemical cause of this effect has not been investigated.

Coating Thickness, Phase II

Coating thickness and thickness variation for Phase II sample set A are shown in Figures 3,4.

Attempts were made to keep coatings in the same thickness range, in order to eliminate the role of thickness in coating performance. However, because coatings were applied according to common practice and with aesthetic requirements for artwork in mind, variations in end thickness occurred. The wax coating was significantly thinner on all substrates, as it would be in real practice. The Nikolas acrylic/acrylic urethane was thicker than the other coatings, especially on bronze, which could have boosted its performance a bit. This coating was in the recommended thickness range and had a satisfactory appearance. It should be noted that the recommended film thickness for most coatings is 1.5-2.0 mil, while it was found in the case of Incralac and the BASF acrylic urethane that much thinner coatings, around 0.6-1.0 mil, resulted from efforts to avoid orange peel and a glossy, "plastic appearance."

Although dry film thickness of Phase II samples shows variation, results are representative of real practice and thus impose a realistic "thickness factor." It is noteworthy that results of coating thickness in both Phase I and Phase II clearly indicate that Incralac is commonly applied well below the recommended manufacturer thickness. As noted in previous reports, the large standard deviation of coatings on the copper roof substrates was due mainly to the uneven patina. Standard deviation in coating thickness was also noticeably increased by brush coating vs. spray coating. Average coating thickness was also obtained for sample set B after weathering, but was not found to vary significantly from results for sample set A.

Adhesion Before and After Weathering. Phases I & II

Cross-cut and X-cut adhesion tests for Phase I samples were re-evaluated in order to increase consistency of results between different operators. Results are shown in. Figures 5,6. Slight adjustments were made in some cases; however, an error was found in the case of adhesion of StanChem waterborne acrylic urethane before weathering on polished, cast bronze. The initial adhesion rating for this coating was a four, not a zero (where 5 optimal adhesion), as previously reported. It was confirmed, however, that adhesion of this coating after accelerated and outdoor weathering fell- to zero. Adhesion rating checks also uncovered that the CCR waterborne polyurethane on polished, cast bronze has undergone aging in the laboratory/storage. The adhesion in this case was reported correctly initially as zero, but changed over time, without exposure to weathering tests, to a rating of five. Adhesion of the polyurethane to polished bronze also changed to a five after accelerated and outdoor weathering. It was observed that the polyurethane films have become extremely tough, so that it is hard to cut through with a scalpel.

Adhesive failure in the wax coatings was somewhat different in nature from the other coatings. Here failure was primarily cohesive, i.e., in the coating layer itself, complicating interpretation and inspection of the test results, especially for very thin wax coats. After weathering, the wax coatings showed an increase in adhesion, possibly due to hardening of the wax. In addition, the Nikolas two-part acrylic/acrylic urethane coatings showed partly interlamellar adhesive failure, primarily before weathering, which decreased the initial ratings.

Results reveal that the Incralac series coatings on polished bronze, except for Incralac with Tinuvin 292, showed a decrease in adhesion after weathering, going from a fair to poor rating. The thick Incralac coating showed the largest drop in magnitude, which may be attributed to poorer mechanical response to thermal shocks during freeze-thaw cycling or to residual stress in the coating. It is particularly interesting that these samples show a larger decrease in adhesion after outdoor weathering than after accelerated weathering. Further investigation of the interfacial chemistry by ATR may shed light on this effect.

Results also show that the organosilane did not consistently increase adhesion of various coatings on polished bronze. In general, this particular silane was found to be a poor choice as a pretreatment because it turned brown and most likely caused crosslinking in coatings. The PPG manufacturer's pretreatment on bronze, used with the PPG acrylic urethane, increased adhesion dramatically, showing the importance of a chemically clean, slightly roughened surface for good adhesion.

X-cut adhesion ratings for Phase I coatings on the unblasted copper roof substrate (Figure 6) are in most cases initially higher than on bronze, except, notably, the waterborne acrylic urethanes. These higher values may be interpreted as due to the large mechanical adhesion factor contributed by penetration of a coating into a patina, and thus the creation of a polymer/mineral matrix, or simply the larger surface area available for contact. The resulting patina colors, which vary dramatically with different coatings, appear to provide visual evidence of coating. Measurements of the combined coating and patina thickness, compared to the same coatings on bronze (see 1996 NCPTT Final Report), confirmed that darker samples corresponded to more coating penetration, and thus saturation, and lighter samples to less penetration. This explains well the initial poor adhesion of the waterborne acrylic urethane coatings on copper roof, which are light in color. Results also show that the Nikolas acrylic/acrylic urethane coatings exhibit worse initial adhesion on copper roof than Incralac, while the opposite was true on polished bronze.

In general, results show very little change in adhesion ratings for coatings on copper roof before and after weathering, with the exception of B-48. In the latter case the adhesion virtually dropped to a rating of zero after outdoor weathering. Adhesion results for Phase I are also discussed in the "Interim Report to the NCPTT 1997 Grant Program."

Results of cross-cut and X-cut adhesion tests for Phase II samples, before and after accelerated weathering, are shown in Figures 7,8. Results first of all show deceptively high ratings for the wax coating on all substrates both before and after weathering. This may be explained as difficulty in observing cohesive failure in the very thin wax coatings applied to Phase II samples, although this type of failure was observed in the thicker wax coatings of Phase I and most likely predominates in wax coatings. The remaining coatings on polished bronze show fairly good to excellent initial adhesion both before and after weathering, with the exception of the Nikolas waterborne acrylic urethane. In the case of Incralac and the Nikolas acrylic/acrylic urethane coatings, initial adhesion values before weathering are higher than in Phase I. This may be attributed to the slightly rougher polish finish on samples in Phase II, and the use of water polishing to produce cleaner surfaces. Both of these coatings also show a decrease in adhesion after weathering. This effect was observed only for the Incralac series coatings on bronze in Phase I, and cannot be explained for the Nikolas coating at this time other than possible differences in surface and coating preparation, or nternal stresses resulting from application. Results also clearly indicate that adhesive failure was generally more prevalent in coatings on the artificially patinated bronze surface.

Initial adhesion ratings on the water-washed and walnut-shell-blasted copper roof substrates (Figure 8) are similar to those on bronze, except for the Nikolas waterborne acrylic urethane and BASF acrylic urethane on blasted copper roof In contrast to results from Phase I, the Nikolas acrylic/acrylic urethane held good adhesion after weathering on the water-washed copper roof, but less so on the blasted substrate. Otherwise, the adhesion of the coatings on both copper roof substrates generally maintained fairly good levels or even increased after weathering.

ELECTROCHEMICAL IMPEDANCE SPECTROSCOPY (EIS)

Electrochemical test methods, primarily EIS, have recently moved center stage as important tools for the quantitative characterization of coatings on metal substrates.[16] EIS is particularly valuable for the rapid ranking of coatings and prediction of future performance. EIS is being used in this study as a parallel technique for coating evaluation.

- Preliminary EIS work was conducted on five polished, cast bronze samples from Phase I. The five coatings tested were: a waterborne acrylic urethane (StanChem, Inc.), Incralac, Incralac + wax, BTA pretreatment + Incralac, and BTA pretreatment + wax. The following results are taken from an internal report by Jamie Welton from the laboratory of Dr. Gordon Bierwagen.

Qualitative impedance values for coating ranking are as follows: good to excellent = values of to greater than 10^9 to greater than 10^{12} Ω cm^2 maintained after two weeks immersion; fair to good = values of 10^6 to greater than 10^9 Ω cm^2 maintained after 2 weeks immersion; poor = values of less than 10^6 Ω cm^2 that do not maintain even this level of protection in immersion. Visual changes to the samples during testing were noted but not taken into account in the rankings. Results were as follows.

Prior to the first EIS, all coatings were clean, and had no pits. The most evenly coated areas were chosen. On the initial run, StanChem waterborne acrylic urethane was the best coating, at approximately 8* 10^7 Ω cm^2, followed by, in order of performance, Incralac (1* 10^7 Ω cm^2), Incralac + wax (4* 10^6 Ω cm^2), BTA + incralac (4* 10^6 Ω cm^2), and BTA + wax (7* 10^5 Ω cm^2).

After immersion for two days, a thin, foggy film formed over the samples pretreated with BTA. The impedance value for BTA + Incralac increased from about 4* 10^6 to 4* 10^8 Ω cm^2, making it the highest performing coating of the five, and the impedance value for BTA + wax increased from 7* 10^5 Ω cm^2 to 9* 10^6 Ω cm^2. The StanChem waterborne acrylic urethane coating fogged. No change was observed for the samples coated with Incralac or incralac + wax. Following BTA + Incralac, the order of performance was: StanChem waterborne acrylic urethane (3* 10^7 Ω cm^2), BTA + wax (9* 10^6 Ω cm^2), Incralac + wax (5* 10^6 Ω cm^2), and Incralac (9* 10^5 Ω cm2. Apparently, the performance of BTA pretreated samples improved under immersion in Harrison’s solution, although the resulting foggy film altered the appearance detrimentally.

After 15 days immersion, EIS results were as follows. BTA + Incralac was still the best coating (1*10^8 Ω cm^2), followed by BTA + wax (9*10^6 Ω cm^2), StanChem waterborne acrylic urethane (9*10^5 Ω cm2), Incralac + wax (9*10^5 Ω cm^2), and Incralac (3*10^5 Ω cm^2). Some changes in the appearance of coatings occurred. StanChem waterborne acrylic urethane was heavily pitted, seriously altering the appearance of the coating. Incralac + wax had two small pits. The sample coated with Incralac alone had become cloudy. The two samples pretreated with BTA did not change any further in appearance.

After 22 days immersion, all coatings degraded slightly, but still held the same ranking from best to worst coatings. After 29 days immersion, however, the impedance modulus for BTA Incralac fell back to almost the initial level, while that of BTA + wax fell only slightly. At this point the StanChem waterborne acrylic urethane was omitted from EIS measurements since its performance value was far below what is considered to be a poor coating. Also, its appearance was full of pits, with highly corroded areas. Measurements were as follows: BTA + wax, $8.5*10^6$ Ω cm^2; BTA + Incralac, $3*10^6$ Ω cm^2; Incralac + wax, $3.1*10^5$ Ω cm2; and Incralac, $1.2*10^5$ Ω cm^2.

These results first of all confirm the extremely poor performance of the StanChem waterborne acrylic urethane. However, E1S results show a comparatively better ranking for the BTA + wax coating than that obtained after accelerated or outdoor weathering in either Phases I or II (see below). This may be related to the overall surface etching and oxidation observed on waxed-only bronze samples after both accelerated and outdoor weathering, suggesting that the wax is particularly susceptible to acid permeation and attack at pH in the range of 3.0-4.0. Acidity was comparatively mild in the EIS tests, i.e., about 5.5-6.0, so that this effect may not be observed.

EIS results also much more strongly indicate a benefit in performance from BTA pretreatment: the two coatings with this pretreatment receive a “fair to good” rating, although a foggy film formed which appeared to correspond to the performance augmentation. This foggy film was not observed in outdoor or accelerated weathering tests. Further EIS testing is necessary in order to confirm whether the benefit observed from BTA pretreatment is temporary in nature and/or related to specific weathering conditions. In addition, EIS showed that the Incralac without BTA pretreatment dropped to a poor rating even though BTA is included in the coating formulation, i.e., BTA inclusion in the coating offered little or no benefit. The ranking order from EIS also showed that a wax topcoat boosted performance, although much less so than BTA pretreatment.

INVESTIGATION OF CU-BTA FILMS ON ROLLED BRONZE BY RAIR

The formation of CuBTA films on rolled bronze was further explored through RAIR. Assuming the applicability of the Beer-Lambert law, which states that absorbance is directly proportional to concentration, the absorbance of the benzene ring breathing vibration at 745 cm^{-1} was used to track the thickness of films obtained after different immersion times in 1.5% BTA/ethanol. Results to date are shown in Figure 9. The different symbols represent individual samples immersed for set lengths of time. The double cross symbols embedded in squares, however, represent one sample with additive immersions, i.e., that was re-immersed for the total periods of time indicated and then analyzed by RAIR. Results shown in this graph, which uses a logarithmic time scale, suggest a direct relationship between the absorbance of Cu(I)BTA films on rolled bronze and time of immersion, following a type of induction period where absorbance remains fairly constant. These results will be confirmed and clarified by work in Phase III (in progress), including investigation of the thickness-immersion time relationships for BTA solutions of different concentrations and solvent type.

R4IR experiments have furthermore shown that Cu(l)BTA films are formed on uncleaned rolled bronze, and measure similar absorbance, i.e., thickness, to that on the solvent-cleaned side. In addition, after coating a sample of rolled bronze with Incralac and then removing the polymer film, clear evidence was obtained by RAIR that a Cu(I)BTA film remained. This film was in the same absorbance range as those obtained from 1-5 minute immersions in BTA/ethanol solutions. Heating of CuBTA films on rolled bronze furthermore showed that the films were stable up to 155 °C.

OVERALL PERFORMANCE AND FAILURE RATINGS

Coating performance evaluation, Phase 1, set lB (accelerated weathering)

Failure ratings were recalculated for results obtained after both 1200 hours and 6 months total accelerated weathering according to methods described in “Experimental Methods” and are shown in Figures 10, 11. The new rankings do not markedly differ from those previously reported, but are believed to be more precise. Comparison of Figures 10 and 11 is especially interesting in respect to apparent differences in rates of failure. For example, after 1200 hours of weathering, most of the coatings in the Incralac series were performing only slightly worse than the Nikolas acrylic/acrylic urethane or single acrylic urethane coatings. But after 6 months of weathering, performance of the Incralac coatings was clearly lagging behind the others. This was also true for thick Incralac, showing that coating thickness was not the overriding factor in performance. However, two of the Incralac coatings, BTA pretreatment + Incralac + wax, and Incralac with silane, were doing somewhat better after 6 months, although still not as well as the Nikolas series. These results indicate a definite benefit from the coupling of BTA pretreatment and a wax topcoat. The addition of silane to the incralac may have caused some crosslinking in the coating, although this was not confirmed. This could have boosted performance, although crosslinking may not be desirable from the standpoint of removability.

Comparison of the Nikolas acrylic and acrylic/acrylic urethane systems after 6 months further suggests that it is the acrylic urethane itself that is boosting performance, with or without the acrylic underlayer (the performance alone of which was comparable to Incralac). The other acrylic coatings based on B-48 did not show any improvement over Incralac despite somewhat increased adhesion ratings. The markedly poor performance of the B-48 resin points out the importance of using a formulated coating, rather than the resin alone. The Nikolas acrylic urethane on bronze clearly outperformed PPG acrylic urethane, which did show, however, a strong benefit from the improved adhesion which resulted from the manufacturer’s pretreatment. The waterborne coatings as a group showed poor performance, as did the wax coatings.

Coating performance evaluation, Phase I, set IC (natural outdoor weathering)

Evaluation of coating performance on sample set IC, Phase I involved the procedure described above. Results are shown in Figure 12. After roughly 1 .5 years of weathering on the roof of the National Gallery of Art in Washington, DC, samples were generally performing well, with the exception of the wax coatings and some acrylics. Results for some samples are unreliable, however, since several mishaps occurred in which samples were knocked or blown over for uncertain periods of time. Some samples were performing noticeably better in natural exposure than accelerated weathering, however, including Incralac with Tinuvin 292, B-48, and the StanChem waterborne acrylic urethane. Again, results did not show any clear benefit from BTA pretreatment under various coatings, but did suggest a boost in performance from BTA pretreatment coupled with a wax topcoat. In general, results of outdoor weathering after 1.5 years correlate reasonably well with results after 1200 hours of accelerated weathering, assuming the latter are somewhat further along in their aging. This suggests that the acceleration factor in this experiment was about 11:1, i.e., 6 months of accelerated weathering predicted performance roughly equivalent to five or more years of outdoor exposure in a similar climate/urban setting.

Coating performance evaluation, Phase I, sets I1B and IIC (accelerated and outdoor weathering)

Failure ratings for coatings on copper roof substrates after 6 months of accelerated weathering are shown in Figure 13. Little or no light green pitting corrosion was produced on the substrates in this weathering regime, and new, dark green or red corrosion was difficult to judge from the top surface. For these reasons, failure ratings were more difficult to obtain than on bronze. It should be noted that corrosion rates on a fresh metal surface are expected to be higher than on an already oxidized/corroded metal, and thus show greater initial change in appearance.

In general, coatings on the 50-year-old copper roof substrates performed reasonably well after *6* months accelerated weathering with notable exceptions. Only one coating clearly failed: the StanChem waterborne acrylic urethane. The superior performance of most coatings on the naturally patinated copper roof compared to that observed on polished bronze may be attributed in part to better adhesion, but more to the reinforcement of a protective corrosion layer. That is, penetration of the coatings into the patina appeared to make the natural patina more protective at this point in the weathering. It must be noted again, however, that appearance of many of these saturated and/or glossy green patinas would be deemed unacceptable from an aesthetic point of view. Results also do not suggest any benefit from BTA pretreatment, but do point to a boost in performance from the wax topcoat alone.

After roughly 1 1/2 years of weathering on the roof of the National Gallery of Art, the majority of coated copper roof samples continued to show little perceptible change in appearance. A small group of exceptions which showed some a noticeable amount of change, in order of best to worst, includes: #9, the B-48 resin; #23, the silicone alkyd; #27, the Nikolas waterborne acrylic urethane; #29, BTA + wax, and #28, wax. Problems observed in these coatings are as follows. The B-48 coating appeared very slightly mottled, with a bit more corrosion at the bottom edge where the sample was touching the wood rack. The Nikolas waterborne acrylic urethane had a slightly mottled appearance, with some corrosion at the bottom. Note that both of these samples had very thin coating applications. The silicone alkyd coating, which was thick and poor in appearance initially, developed whitish areas at the peak of brushmarks in the coating, but showed no signs of corrosion.

In addition, both of the waxed copper roof samples had a comparatively poor appearance. They appeared very mottled, with dark spotting, in addition to severe accumulation of dirt and soot embedded in the coating. Sample #28, without BTA pretreatment, appeared darker and slightly worse than that with the BTA pretreatment. in addition, under magnification, the surfaces of the coatings no longer appeared smooth, but rough amid with opaque patches of bloom. Some flaking was also evident. On #28, at least one pit of light green corrosion was visible.

Only one coating in this group clearly failed: the StanChem waterborne acrylic urethane. This coating turned very yellow with flaking and all-over cracking, as well as dark green mottling under the coating.

Coating performance evaluation, Phase II, set B (accelerated weathering)

Final evaluation of coating performance in Phase II is not complete at this time. After weathering corrosion descriptions are summarized in Table II. Before and after weathering photographs of these samples are attached. Overall order of performance, derived empirically from visual appearance, was as follows. On the polished bronze substrates the order of performance was: Nikolas acrylic/acrylic urethane/wax > Incralac/wax > BTA/BASF acrylic urethane/wax > Nikolas waterborne acrylic urethane/wax > BTA/wax > silane/wax > uncoated. The unwaxed Incralac sample did exhibit slightly more pitting corrosion than the waxed samples, and it was noted that sample IlBb, on which the Incralac was thicker, had slightly improved performance. On the patinated bronze substrates, overall coating performance was markedly worse, and the ranking order was notably different: Nikolas waterborne acrylic urethane/wax > Incralac/wax > BTA/BASF acrylic urethane/wax ≥ Nikolas acrylic/acrylic urethane/wax > BTA/wax > uncoated. The superior performance of the waterborne coating on this particular substrate was surprising, and will be investigated further.

On the unblasted copper roof (water-washed only), apparent order of performance was: Incralac/wax ≥ Nikolas acrylic/acrylic urethane/wax > BTA/BASF acrylic urethane/wax > Nikolas waterborne acrylic urethane/wax > BTA/wax> uncoated. On the blasted copper roof substrates, the order of performance again differed: BTA/BASF acrylic urethane/wax > Incralac/wax ≥Nikolas acrylic/acrylic urethane/wax > Nikolas waterborne acrylic urethane/wax > BTA/wax > uncoated. It was noted that on both copper roof substrates, overall performance of the coatings was more varied from substrate to substrate.

Preliminary failure ratings for the coatings on these substrates are shown together graphically in Figure 14. These ratings were computed according the procedure in “Experimental Methods;” they appear to reflect the ranking order of coating performance quite well in all but one case: the Nikolas acrylic/acrylic urethane on patinated bronze. This coating peeled severely at the scribemark, but overall, where still adhered, provided fairly good protection to the patinated metal. In this case, the failure rating formula, which is weighted toward evidence of corrosion, does not reflect the dramatic failure in the coating itself very well.

The results are shown in decreasing order of general “group performance,” where the unblasted copper roof samples were the most unchanged after weathering, followed by the polished bronze, the blasted copper roof and tailed by the patinated bronze. On the latter two substrates, the types of performance failure also varied greatly, which the total ratings do not reflect well. The results do illustrate, however, that the degree of failure on the “treated” substrates, i.e., on the blasted copper roof and the artificially patinated bronze, was generally higher. In addition, results highlight the poor performance of the BTA + wax coating on all substrates given this particular weathering regimen.

Results for the uncoated, polished or patinated substrates pretreated with BTA show that BTA by itself has a limited corrosion-inhibiting effect in terms of chlorides and formation of the unidentified black corrosion. However, as discussed above, BTA pretreatment of selected samples in Phase I does not show any clear performance benefit in accelerated or outdoor testing. This suggests that the limited effect of BTA is much less important than that afforded by the coating, and that it may be related primarily to the thickness of the CuBTA film, i.e., the ability of BTA to form an additional barrier at the metal surface. Addition of BTA in the coating formulation, which was shown to allow formation of an extremely thin CuBTA film, may have the most limited efficacy. The “BTA factor” will be further explored in Phase ITT of the study.

Conclusions

Overall, the failure ratings do not correlate to any one property of the coating systems, including adhesion ratings. However, the generally poor adhesion of coatings on patinated bronze does partly explain the poorer performance of coatings on this substrate. On the blasted copper roof substrates, which also had coating performance problems, adhesion ratings were not generally worse than on the unblasted substrate, though. As previously reported, it is clear that adhesion is not an overriding factor in coating performance unless it is very poor or very susceptible to change. It is quite possible, for example, that the drop in adhesion after weathering observed in the Nikolas acrylic/acrylic urethane coatings on all substrates in Phase ii, but not at all in Phase I, explains why this coating was not the front-runner it had been in Phase 1. This underscores the importance, and difficulty, of meticulous, consistent preparation and coating application, which may account for these differences.

Similarly, thickness does not appear to be an overriding factor in performance unless the coating is too thin. For example, the wax coating in Phase ii was significantly thinner than in Phase I, and the coatings stood out as poor performers. However, the poor performance of the wax coatings appeared to also relate to acid sensitivity, as discussed above. In Phase I, it appeared that thickness was less important for coatings on the naturally patinated substrate than was penetration of the coating into the patina. Results also illustrated that the lighter colors achieved from coating application were due to relative penetration into the patina, and vice versa. Coatings which had no significant penetration, including the waterborne coatings and B-48, failed, suggesting that moisture was able penetrate under the coating and get trapped there, causing corrosion. However, this hypothesis does not appear to hold true in Phase ii, presumably because there were other equally important factors at work.

Rather, it appears that the harsher, and more accelerated weathering regimen in Phase II highlighted other important causes of failure. Failure ratings show similar rankings for coatings on polished bronze and unblasted copper roof This appears to be related to inherent properties of the coatings. Significantly, however, results illustrate that walnut-shell blasting cannot be considered as a good or even improved surface preparation from the standpoint of coating performance. Even more dramatically, results show that artificial patination may create an unstable surface, possibly related to the presence of sulfides, which also compromises coating performance. These observations and hypotheses will be investigated in Phase Ill of the study. Results thus far underscore the importance that the substrate and its preparation play in coating performance and thus in coating selection. It remains difficult, if not impossible, to pinpoint any individual factor as key to good or poor coating performance in these complex systems.

Future Work

Coatings of several samples before and after weathering will be examined by SEM for significant changes in morphology, such as the presence of porosity. Several samples have already been carbon-coated for this purpose, but results have not yet been obtained.

Digital images have been made of all samples A and B from Phase II, i.e., samples that underwent either no weathering or accelerated weathering. These images are being utilized for more accurate measurement of linear creepage at the scribemarks and % overall pitting corrosion. The image analysis software, IP Spectrum from Scanalytics, also enables characterization of the pitting corrosion in terms of spot shape and size variation, as well as color change measurements. This quantitative data will be utilized in the overall failure ratings of the samples.

Additional characterization of the chemistry of the bulk and metal/polymer interfaces of all samples will be performed by py-GC/MS, GC/MS, FTIR, ATR, RAIR, and other techniques as necessary. In addition, solubility and removability tests will be performed on Incralac-coated samples from both Phases I and II in order to examine the question of possible crosslinking in the films with aging. It is planned that a complete set of unweathered and weathered samples from Phase II will undergo EIS analysis in the laboratory of Dr. Gordon Bierwagen, North Dakota State University. These results will be interesting to compare to the evaluations obtained in this laboratory after weathering.

Sample set C from Phase II is currently weathering on the roof of the National Gallery and will undergo evaluation as above.

Dr. W.J. van Ooij, University of Cincinnati, will conduct ellipsometry on samples of CuBTA films on rolled bronze from the above experiment in order to correlate actual film thickness with absorbance measurements. Investigation of CuBTA films on rolled bronze by RAIR is continuing in order to confirm trends seen thus far and to examine differences in CuBTA film formation in various solutions and solution concentration. Samples from several Phase II coupons, after accelerated weathering, were examined by Dr. Ralph Mitchell of Harvard University for evidence of microbial-induced corrosion. Dr. Mitchell reported that a large amount of microbial activity was present on all samples. This researcher will be pursuing this subject in the future.

Acknowledgments

This work was made possible through funding from the US Department of the Interior, National Park Service, and National Center for Preservation Technology and Training. Any opinions, findings, conclusions and recommendations expressed in this paper are those of the authors and do not reflect the views of the National Gallery of Art, the US Department of the Interior, the National Park Service or the National Center for Preservation Technology and Training.

Other acknowledgments: chemical, technical and other support, Ross Merrill, Tai-a Shedlosky (Research Assistant), Julia Redman (Summer Intern), Michael Palmer (S.EM1EDS), Lisha Glinsman (XRF), Chris Maines and Siobhan Watts (Py-GC/MS), and Philip Charles, Lorene Emerson, Dean Beasom, James Locke (photography) at the National Gallery of Art, Washington, DC; Dr. Gordon Bierwagen, North Dakota State University; Dr. W.J. van Ooij, University of Cincinnati; Dr. George Wheeler, Metropolitan Museum of Art, New York, NY; coatings application, Cameron Wilson, Brooklyn, NY and Andrew Baxter (Bronze et al), Richmond, VA; bronze samples, Bedi-Makky Foundry, Inc., Brooklyn, NY; copper roof samples, Barbara Wolanin and the Architect of the Capitol, Washington, DC; coating samples and technical assistance, Buck Nikolas, G.J. Nikolas, Inc., BASF Corporation, StanChem, Inc.; coating formulation, Cape Cod Research, Inc.

Footnote references

---

[1] See L. Brostoff and E. René de la Pie, “Final Report to the NCPTT 1996 Grant Program: Research into Protective Coating Systems for Outdoor Bronze Sculpture and Ornamentation. Phase I.”

[2] Society of American Engineers, Accelerated Exposure of Automotive Exterior Materials Using a Controlled Irradiance Water Cooled Xenon Arc Apparatus, *SAE J1960*. June 1989: ASTM D3459. D2243.

[3] Based on Nassau, K. et al., “The reaction of simulated rain with copper, copper patina, and some copper compounds,” and Graedel, T. E., “Copper patinas formed in the atmosphere-II. A qualitative assessment of mechanisms,” in Special Issue: Copper Patina Formation Corrosion, *Corrosion Science*, Vol. no. 27. no. 7, 1987.

[4] See for example Suga, S. and Suga, S., “Development of Simulated Acid Rain Test Using CCT Method,” Accelerated and Outdoor Durability Testing of Organic Materials, ASTM STP 1202, Warren D. Ketola and Douglas Gorssman, Eds., American Society for Testing and Materials, Philadelphia, 1994, pp. 247-262.

[5] Pierce, Percy E. and Schoff, Clifford K., Coating Film Defects (Federation Series of Coatings Technology, Philadelphia, Pa., January 1988), pp. 11-20.

[6] Depth of penetration, d_p, was calculated as follows: $[d_p\ ?_l/2p[\sin^2 a - (n_2/n_1)^2\}^{1/2}$**},** where a is the angle of incidence, $?_l$ the wavelength of radiation in the optically denser medium, and n_1 and n_2 are the refractive indexes.

[7] Perfetti, Bruno M., Metal Surface Characteristics Affecting Organic Coatings (Federation Series of Coatings Technology, Blue Bell, Pa., August 1994), p. 63.

[8] Technical Data Bulletin, 11565 OD Lacquer RFU. G.J. Nikolas & Co., Inc., 5/24/96.

[9] Ibid., pp. 239-265.

[10] BTA is often referred to as a UV absorber. In many instances, it is unclear whether manufacturers are referring to the benzotriazole class of UV absorbers or to ETA itself. in the case of this coating, however, discussions with Mr. Buck Nikolas disclosed that BTA proper is an ingredient in the coating.

[11] Nassau et al., “The Characterization of Patina Components by X-ray Diffraction and Evolved Gas Analysis,”

Corrosion Science Vol. 27, No. 7 (1987), pp. 669-684.

[12] T.E. Graedel et al., “Copper Patinas Formed in tile Atmosphere-I,” Corrosion Science Vol. 27, No. 7 (1987), pp. 639-657; L.S. Selwyn et al., “Outdoor Bronze Statues: Analysis of Metal and Surface Samples,” Studies in Conservation 41(1996), pp. 205-228.

[13] Rhom and Haas technical literature.

[14] Hare, Clive H., Protective Coatings: Fundamentals of Chemistry and Composition (Technology Publishing Co., Pittsburgh, Pa., 1994), p. 248.

[15] Cf. for example S.G. Croll, “The Origin of Residual Internal Stress in Solvent—Cast Thermoplastic Coatings,” J. Applied Polymer Sci., Vol. 23 (1979), pp. 847-858; Hare, Clive H., “Internal Stress-Related Coating System Failures,” J. Protective Coatings and Linings, Vol. 13, no. 10 (Oct. 1996). pp. 99-135.

[16] See, e.g., Bierwagen, Gordon, “Recent Developments in Coatings Science in Corrosion Control and Durability: Implications for Art Conservation,” in AIC Abstracts, 25th Annual Meeting, June 9-15, 1997, San Diego, Ca., pp. 7-9; Murray, John N., “Electrochemical test methods for evaluating organic coatings on metals: Part I. Introduction and generalities regarding electrochemical testing of organic coatings,” Progress in Organic Coatings 30 (1997), pp. 2225-233.

Table I

Key to Coatings

Phase I

1. Incralac (Inc)
2. Benzotriazole (BTA) pretreatment (pt) + Incralac
3. Incralac + wax
4. BTA + Incralac + wax
5. Incralac w/Tinuvin 292 (Tin)
6. Incralac w/silane (sil)
7. silane pt + Incralac
8. thick Incralac
9. B-48
10. CCR acrylic
11. silane pt + CCR acrylic
12. Nikolas (NK) acrylic 11565 (acr)
13. PPG acrylic DAU 468
14. PPG acrylic DAU 468 + acrylic urethane (au) DAU 75
15. NK acrylic 11565 + acrylic urethane 9778 + wax
16. BTA pt + NK acrylic 11565 + au 9778
17. silane pt + NK acrylic 11565 + acrylic urethane 9778
18. NK acrylic 11565 + acrylic urethane 9778 + wax
19. NK acrylic urethane 9778
20. PPG acrylic urethane DAU 75
21. manufacturer’s pt + PPG acrylic urethane DAU 75
22. silane pt + NK acrylic urethane 9778
23. CCR silicone slkyd (SiAlkyd)
24. CCR waterborne polurethane (polyur)
25. silane (2% gamma APS) pt
26. StanChem (SC) waterborne acrylic urethane (wbau)
27. NK waterborne acrylic urethane 11560
28. Veloz wax (Vwax)
29. BTA pt + Veloz wax
30. Control
31. BTA pt + CCR acrylic
32. silane + CCR polyurethane
33. BTA
34. Control

Phase II

1. Incralac + wax
2. TA pt +wax
3. Nikolas acrylic 11565 + Nikolas acrylic urethane 9778 + wax
4. BTA pt + BASF acrylic urethane 923-85 + wax
5. kolas waterborne acrylic urethane 11560 + wax
6. Control (C w/ BTA pt)

Table II
Coating and Corrosion Descriptions after Accelerated Weathering, Phase II

Sample	**Polished Bronze**		**Patinated Bronze**		**Copper Roof**		**Walnut shell-blasted Copper Roof**	
Corrosion Area	surface a	scribe b	surface c	scribe d	surface e	scribe f	surface g	scribe h
1- Incralac + wax	Small amounts of waxy green corrosion. Blistering from underneath the coating. Powdery corrosion on a broken blister. Surface. Spotting Orange peel.	Bright green corrosion.	Light green waxy spots under and through coating. Little blisters around the larger spots. Darker brown around those areas. Black streaks under magnification. Orange peel. Cratering.	Medium green, some blisters forming around the X.	Surface spotting Light orange peel	Light green powdery corrosion	Areas of black. Darkened, brown green areas. Coating darkened. Orange peel Surface spotting.	Powdery green. A halo of dark area around the scribe mark.
2- BTA + wax	Many bright spots of powdery green corrosion. Black lines on surface of the coating. Color changed/iridescent film.	Small amounts of green corrosion.	Green and light powdery green corrosion spots. Surface has darkened to a purple brown color with streaky spots.	Medium green corrosion.	Heavy light green powdery corrosion spots. Some yellow green spots.	Spotty light green, powdery corrosion. Does not fill the scribe mark.	A lot of bright green, powdery corrosion.	Bright, light green corrosion.
3-NK urethane + wax	Very small amounts of green corrosion. Surface spotting and cratering.	Bright green corrosion that fills the X.	Iridescent film. Tiny white spots under magnification. (A visible layer under the coating). Cratering and seeding.	Sever peeling around the scribe. Green corrosion in the scribemark. Dark areas around parts of the scribe. Small blisters around the scribe.	Yellowed. Surface spotting. Streaking or whitening in the coating layer.	Light green powdery corrosion filling the scribemark.	Light green & white powdery corrosion. Darkened area towards the bottom of the plate. Light orange peel.	Light green corrosion. Dark halo around the X. Some powdery white corrosion.
4- BTA + BASF acrylic urethane + wax	Very small amounts of green corrosion. Surface spotting. Cratering.	Bright green corrosion outlined by a dark area outside the scribe mark.	Surface covered in small white blisters. Hazing. Some pitting.	Filled with green corrosion, surrounded by small blisters.	Yellow powdery spots. A bit of green corrosion. Surface spotting. Whitened appearance.	Powdery light green corrosion.	Waxy light green spots of corrosion. Darkened in areas Seeds	Green corrosion.
5- NK waterborne acrylic urethane + was	Small spots of waxy green corrosion surrounded by dark areas. Tiny pox marks in the surface of the bronze. Solvent popping/air entrapment.	Green powdery corrosion. Coating starting to peel around scribemark.	Spots of green waxy corrosion. Corrosion blisters. Cratering and seeds.	Yellow green powdery corrosion.	Yellowed. Surface spotting. Uneven dark areas. Air entrapment.	Dark halo around the scribe. Green corrosion filling the scribemark.	Spots of yellow-green corrosion. Small spots of blue corrosion. Dark area around edges. Water spotting.	Green corrosion in the scribe Dark halo around the X.
6- No Coating	Black streaks of charcoal like corrosion. Black and dark brown spots. Good sized green corrosion spots. Reddish-brown corrosion exists where black is not overlapping. Area of white spots Bottom of plate very dark.	N/A	Dense black charcoal-colored corrosion. Iridescent reflection. Brown patina remaining at edges. Small spots of green corrosion.	N/A	Black charcoal-colored corrosion. Darker green area towards the bottom. Tiny spots of green corrosion. Brownish yellow corrosion. Dark areas.	N/A	Dark black spots. Areas of bright green spots. Light white areas. Bright green around black spots. Patina darkened towards the bottom of the plate.	N/A

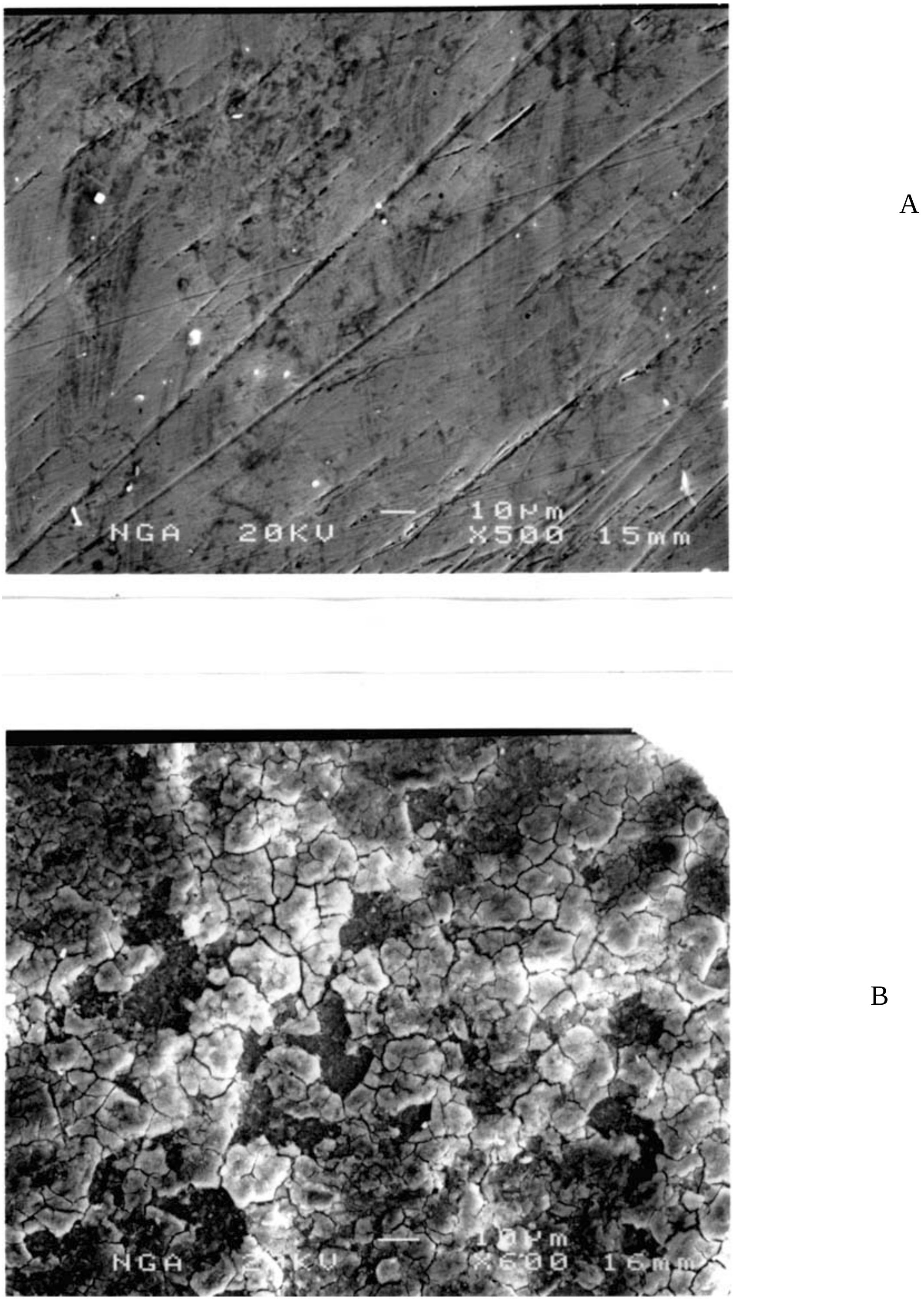

Figure 1: SEM photographs normal image of a) cast bronze (500x) and b) patinated bronze (600x).

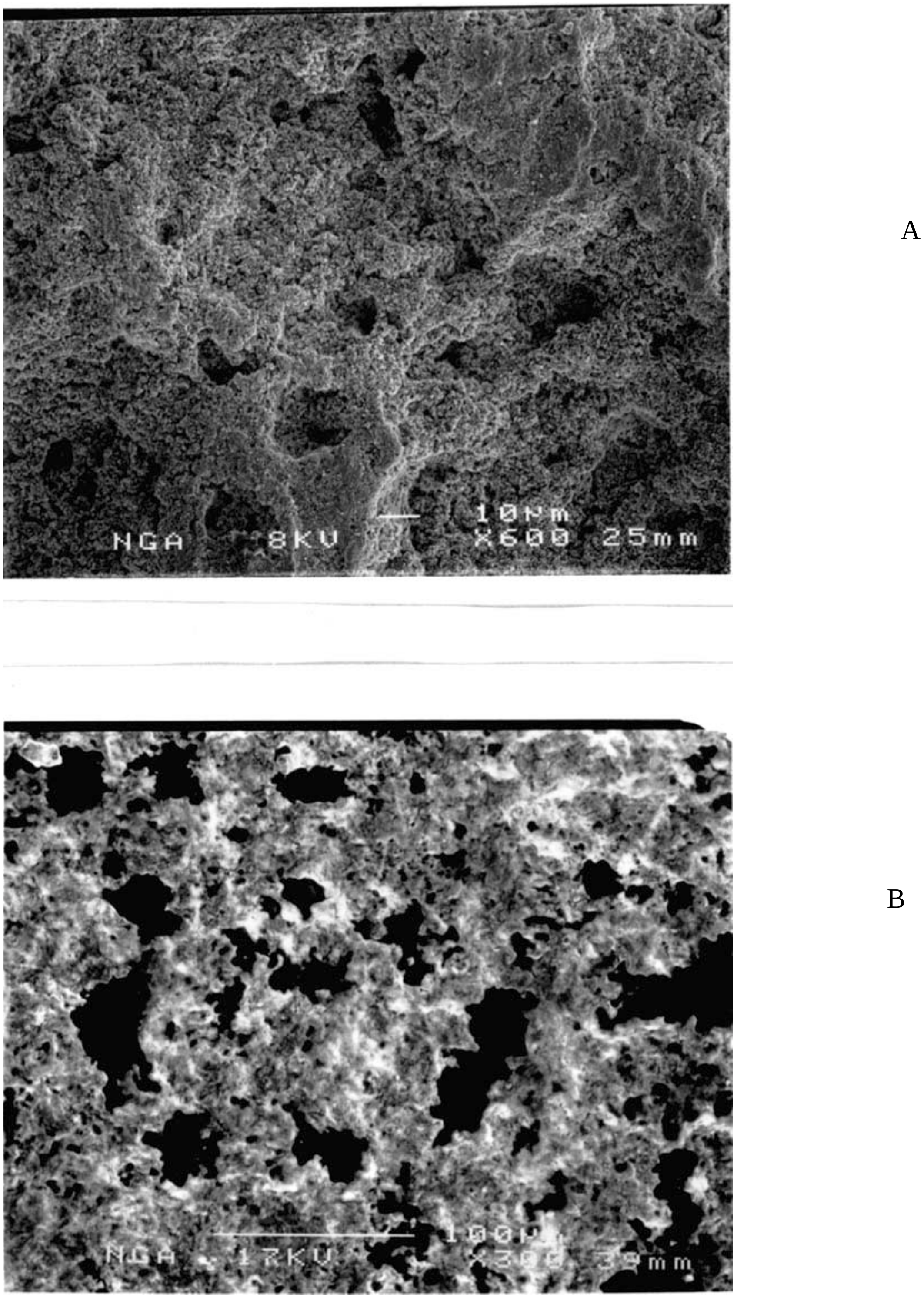

Figure 2: SEM photographs normal image of a) 50-year-old copper roof (600x) and b) 50-year-old copper roof, walnutshell-blasted (300x).

Figure 3

Coating + Patina Thickness and Standard Deviation (sd) on Unweathered Bronze Substrates, Phase II

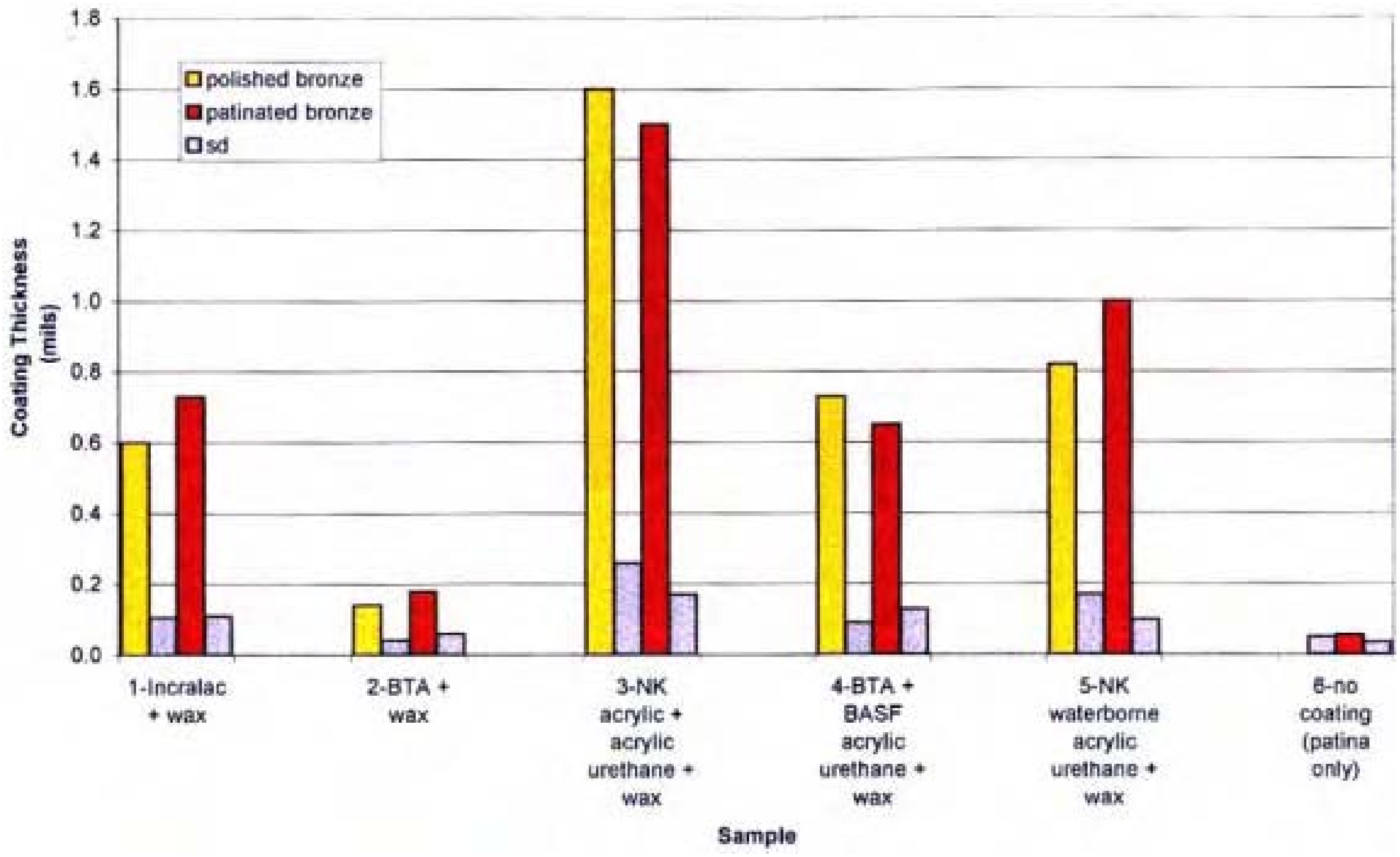

Figure 4

Coating + Patina Thickness and Standard Deviation (sd) on Unweathered 50-year-old Copper Roof Substrates, Phase II Sample

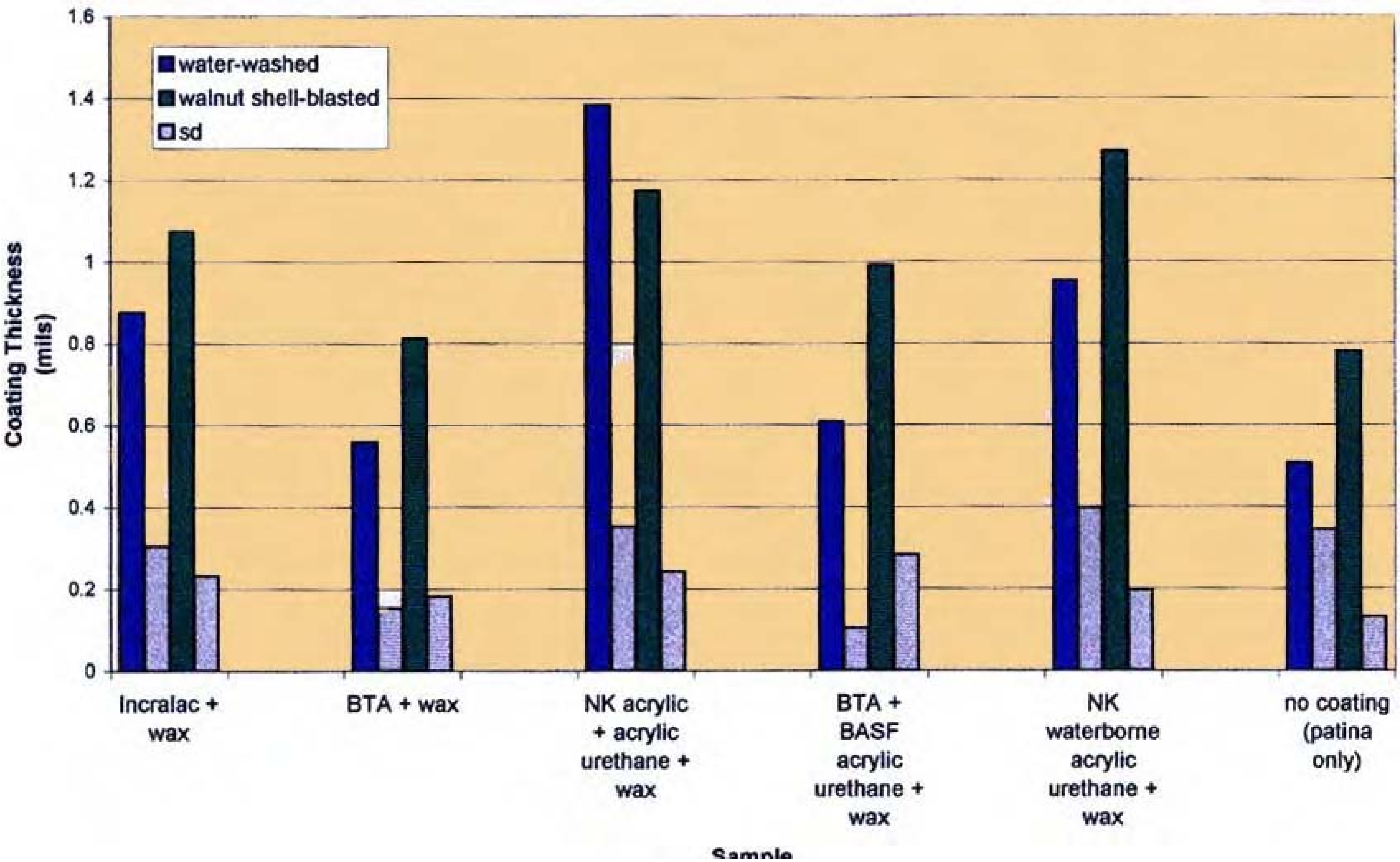

Figure 5

Cross-Cut Adhesion Ratings of Coatings on
Polished, Cast Bronze, Phase I, Before and After Weathering

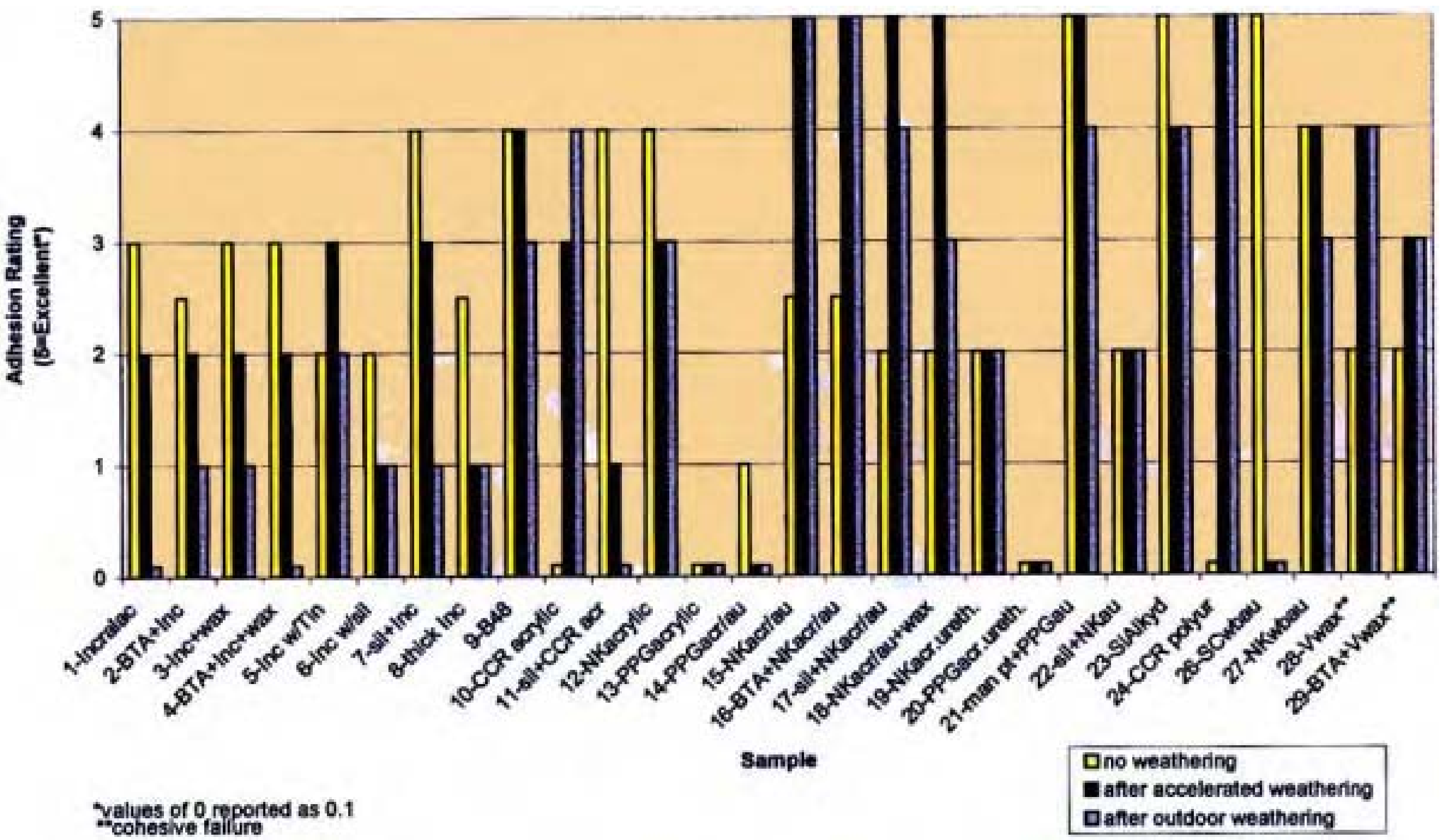

*values of 0 reported as 0.1
**cohesive failure

Figure 6

X-Cut Adhesion Ratings of Coatings on
50-Year-Old Copper Roof, Phase I, Before and After Weathering

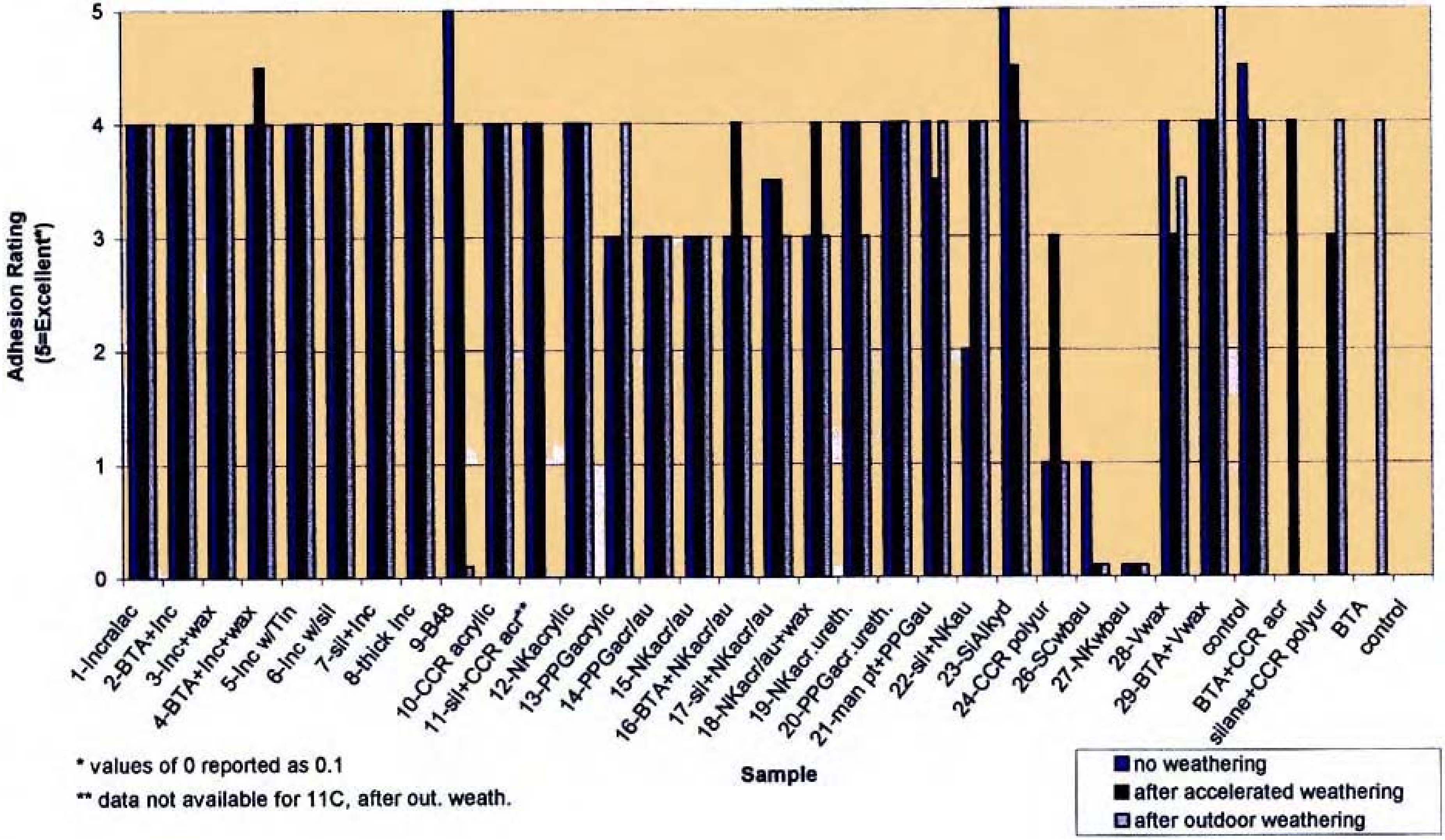

* values of 0 reported as 0.1

** data not available for 11C, after out. weath.

Figure 7

Cross-Cut Adhesion Ratings of Coatings on Cast Bronze, Phase II, Before and After Accelerated Weathering

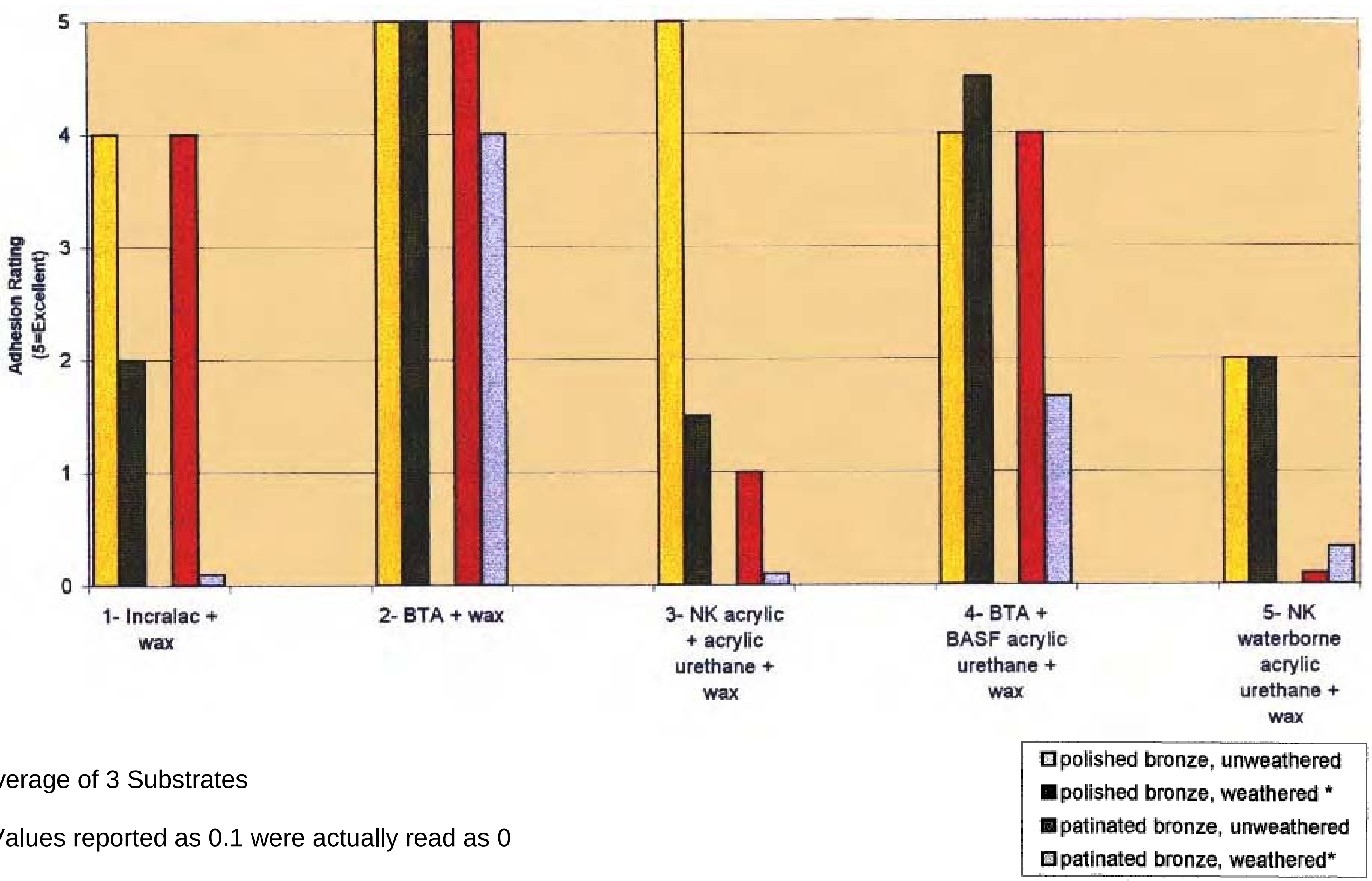

*Average of 3 Substrates

**Values reported as 0.1 were actually read as 0

Figure 8

X-Cut Adhesion Ratings of Coatings on 50-Year Old Copper Roof, Phase II, Before and After Accelerated Weathering

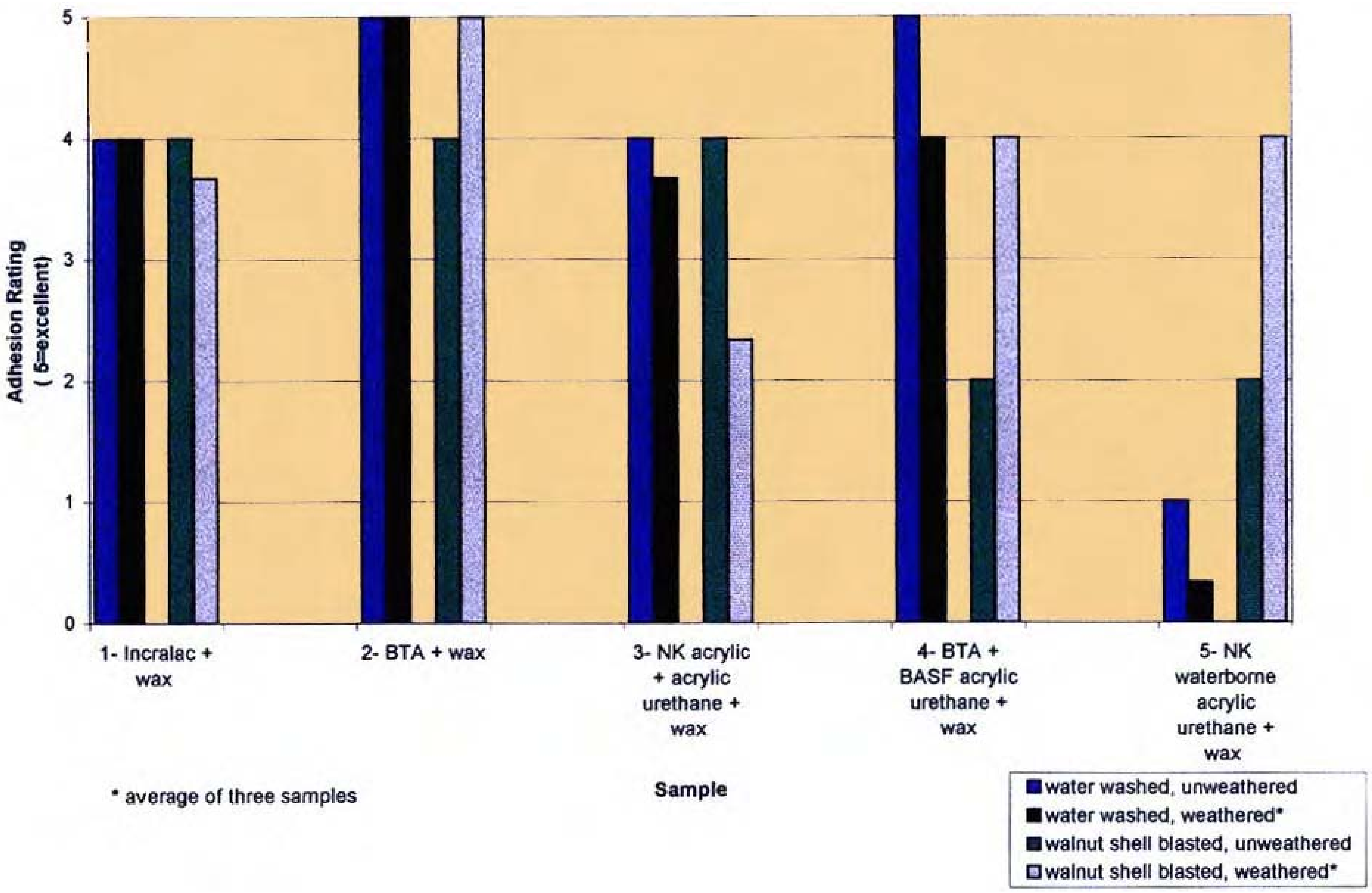

Figure 9

Absorbance of 745 cm^{1} in CuBTA Films
Formed on Rolled Bronze After Immersion in 1.5% BTA/ethanol

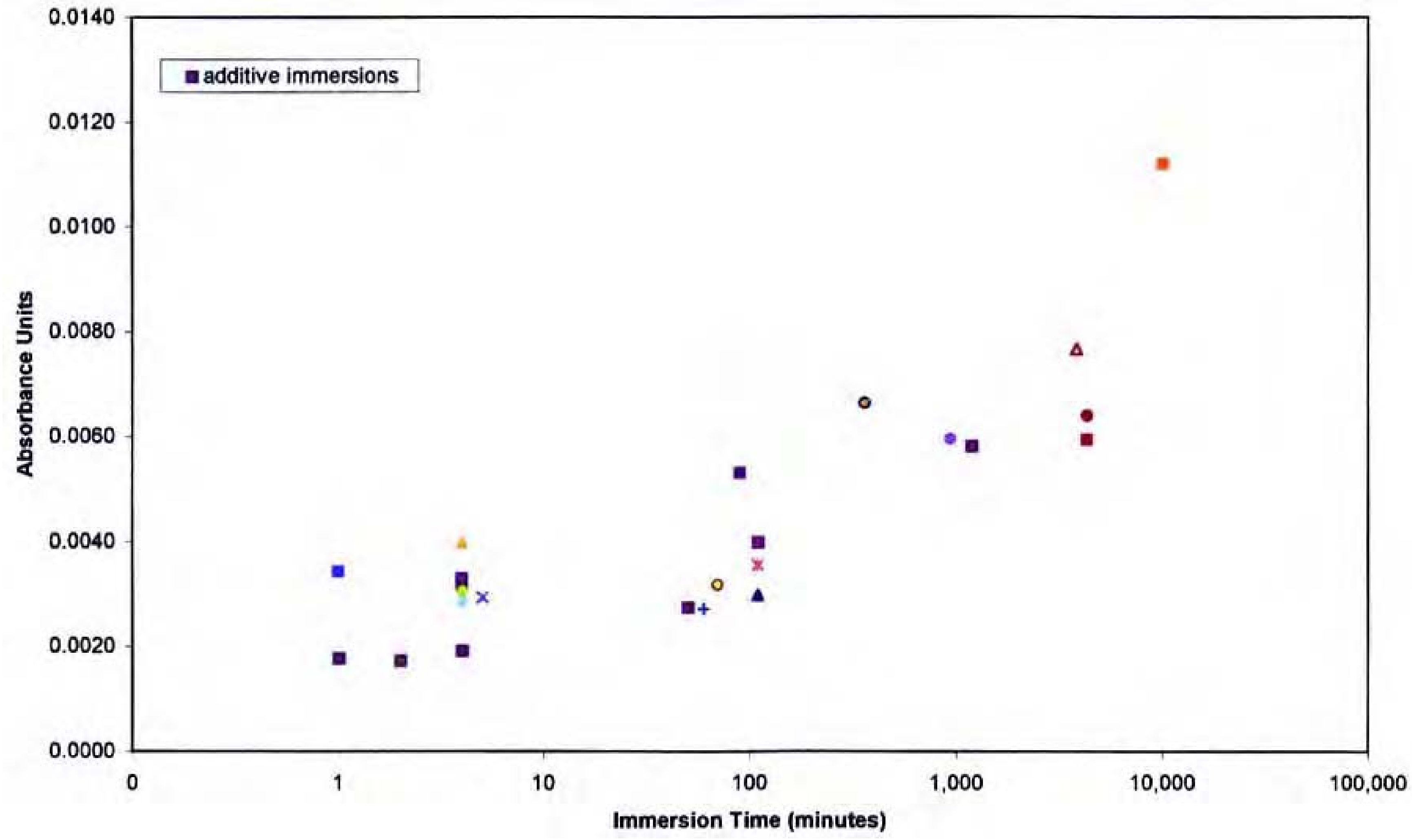

Figure 10

Failure Rating of Coatings on Polished, Cast Bronze, Phase I, After 1200 Hr. Accelerated Weathering Based on Mean Creepage at a Scribemark and % Overall Corrosion

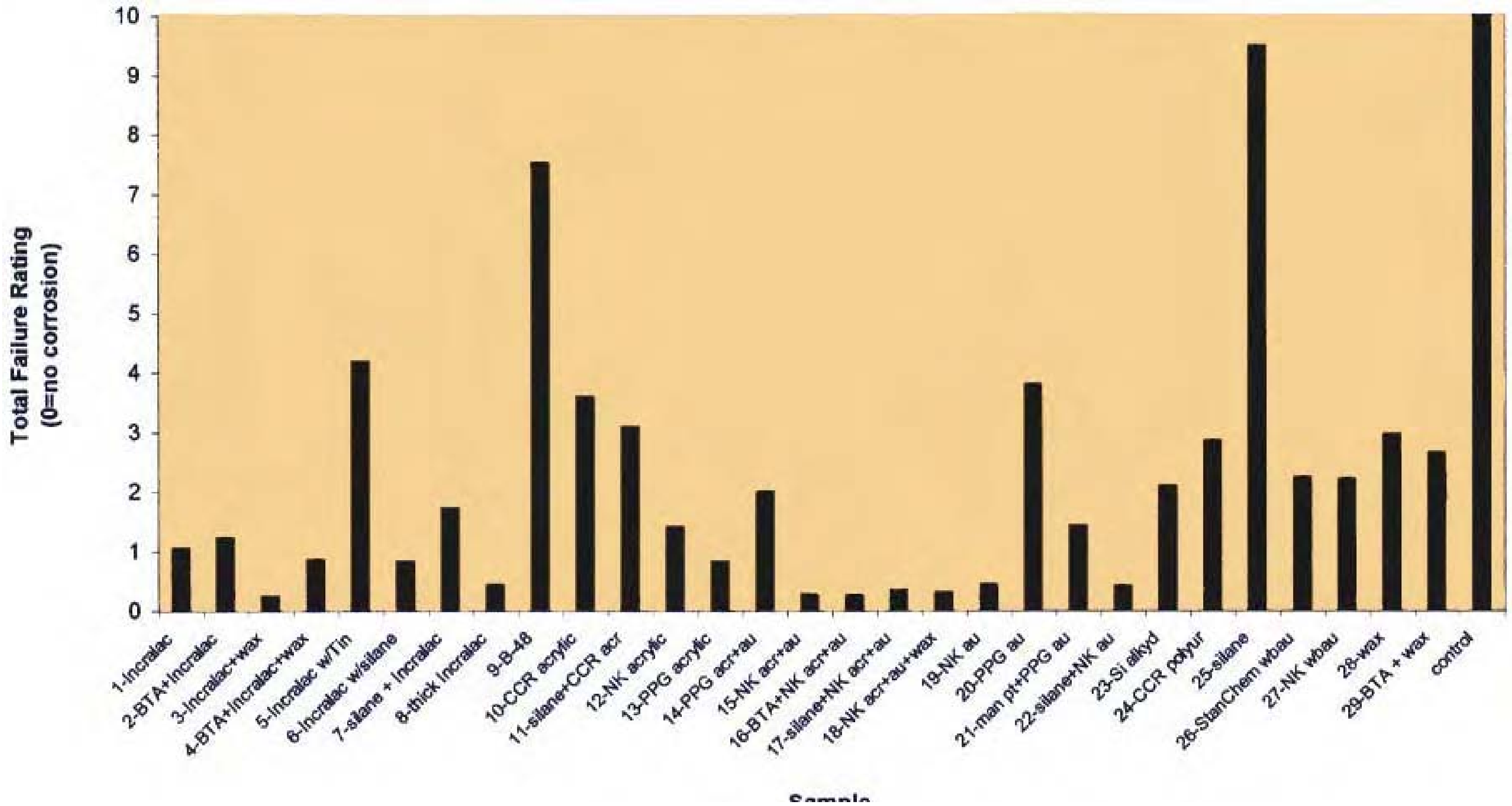

Sample

Figure 11

Failure Rating of Coatings on Polished, Cast Bronze, Phase I,
After 6 Mo. Accelerated Weathering Based on Visual Evaluation of Coating Appearance,
Overall Corrosion, and Corrosion at Scribemark
Sample

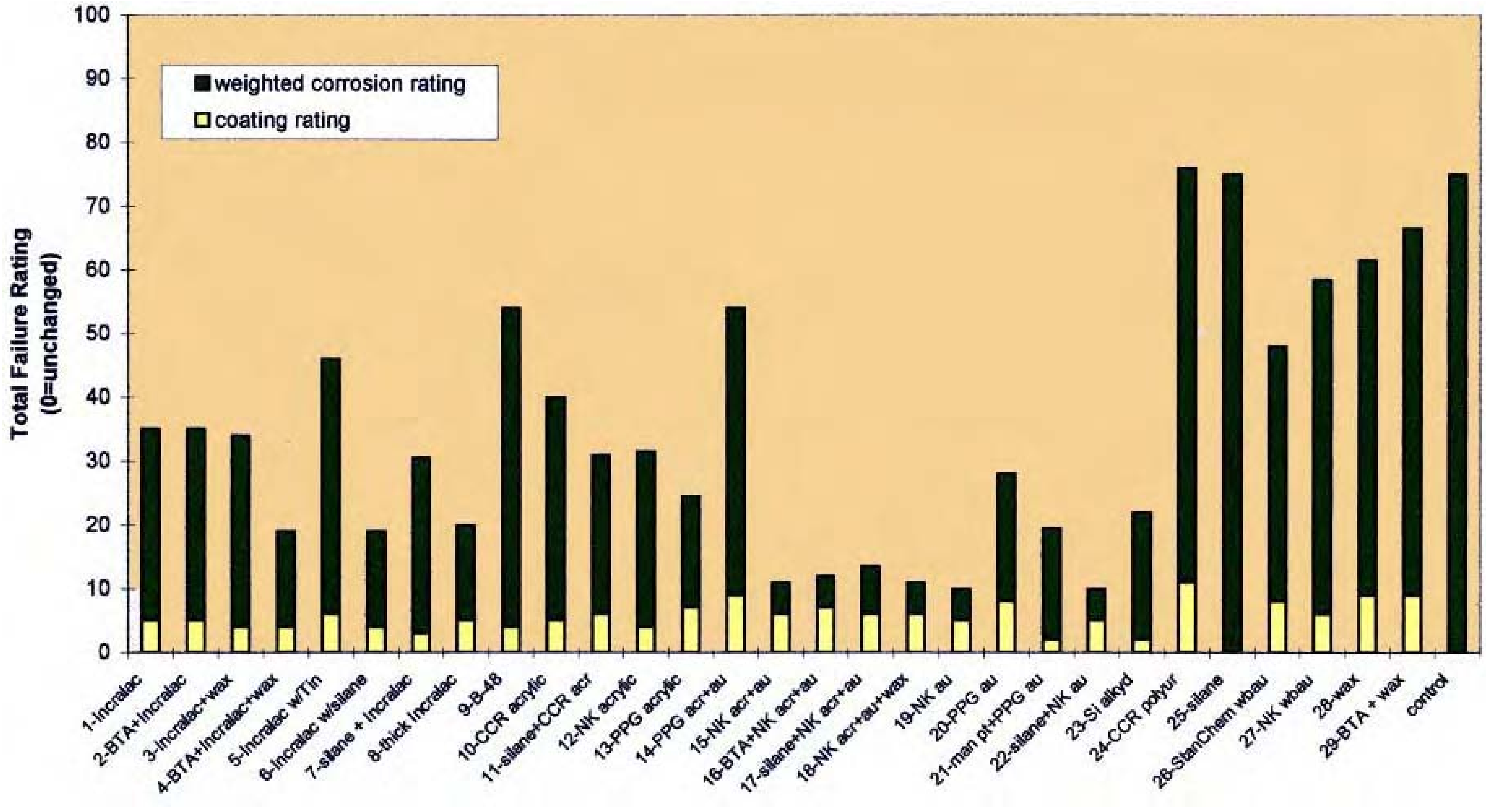

Figure 12

Failure Ratings of Coatings on Polished, Cast Bronze Phase I, After 1.5 Yr. Natural, Outdoor Weathering Based on Visual Evaluation of Coating Appearance, Overall Corrosion, and Corrosion at

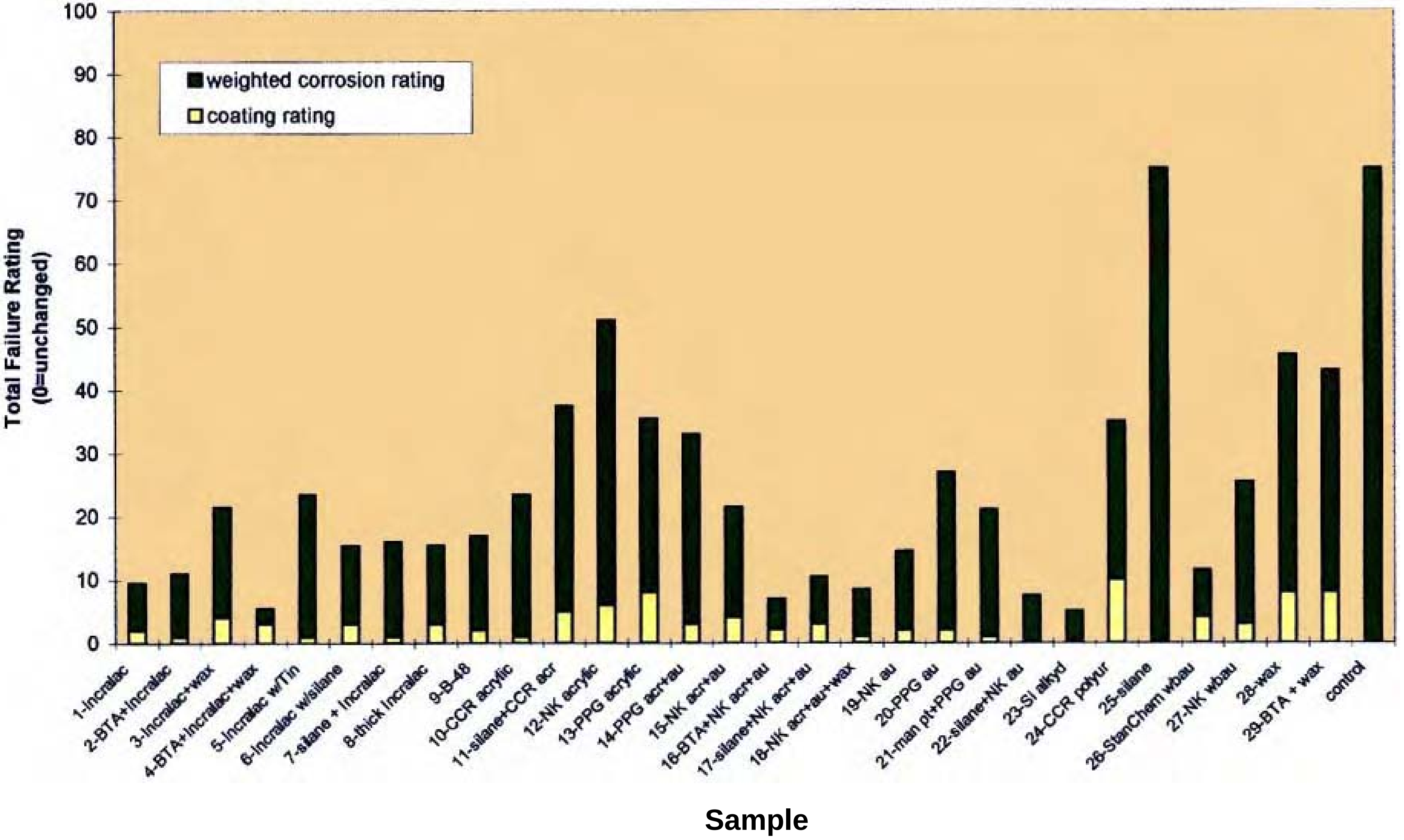

Figure 13

Failure Ratings of Coatings on 50-Year-Old Copper Roof, Phase I, After 6 Mo. Accelerated Weathering, Based on Visual Evaluation of Coating Appearance, Overall Corrosion, and Corrosion at a Scribemark

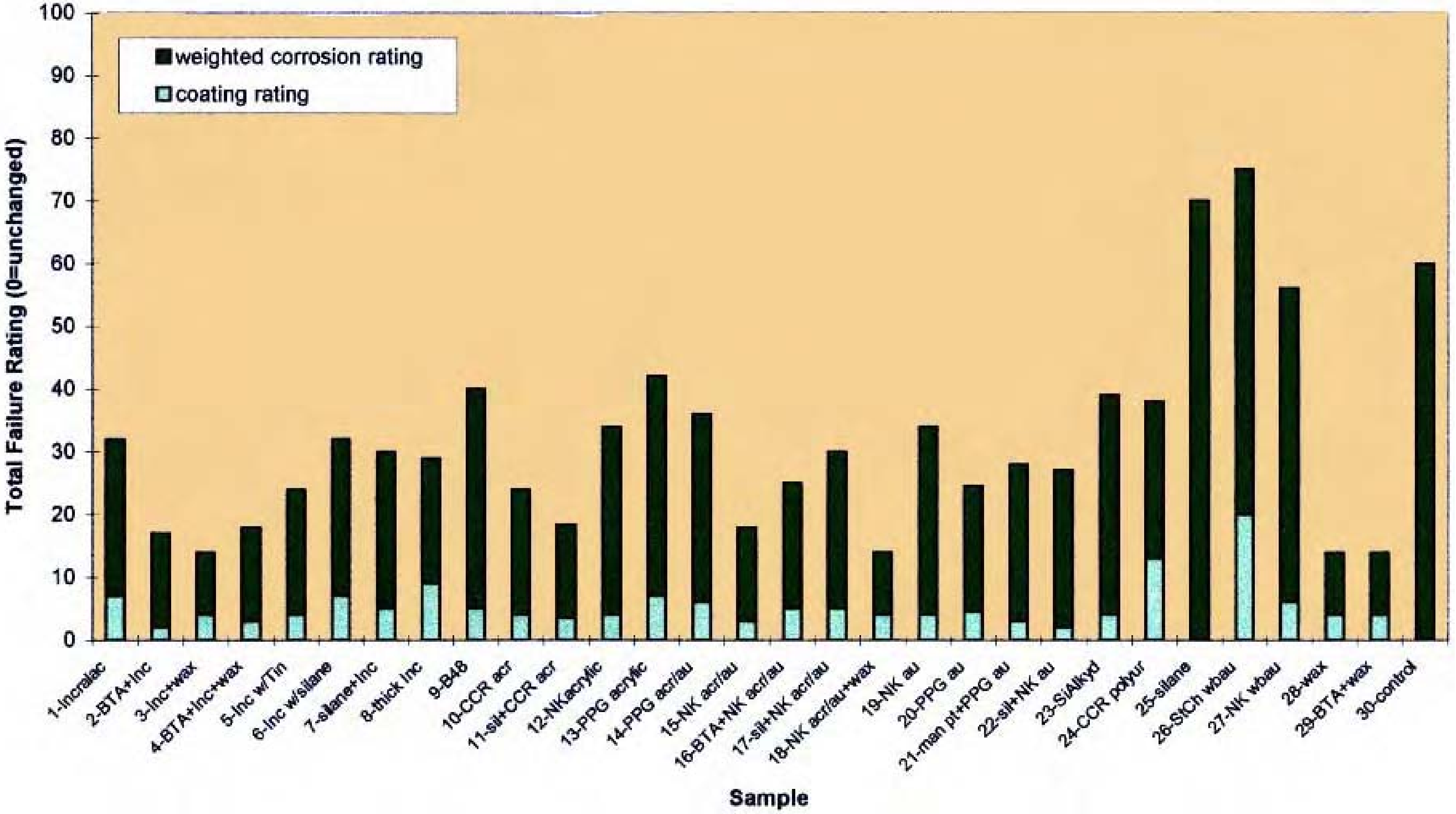

Figure 14

Preliminary Failure Ratings of Coatings on Bronze and Copper Roof, Phase II, after 120 days Accelerated Weathering

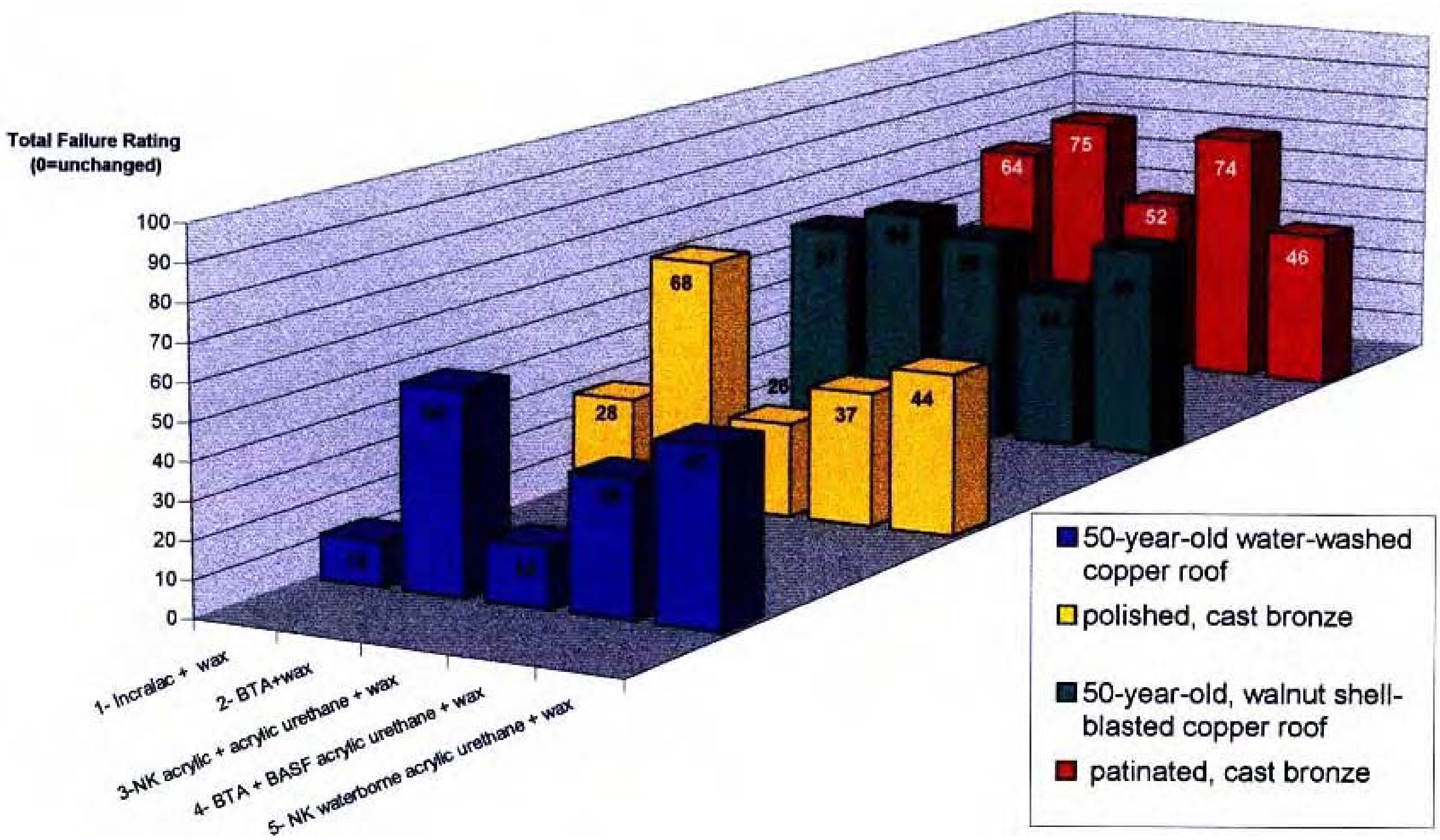

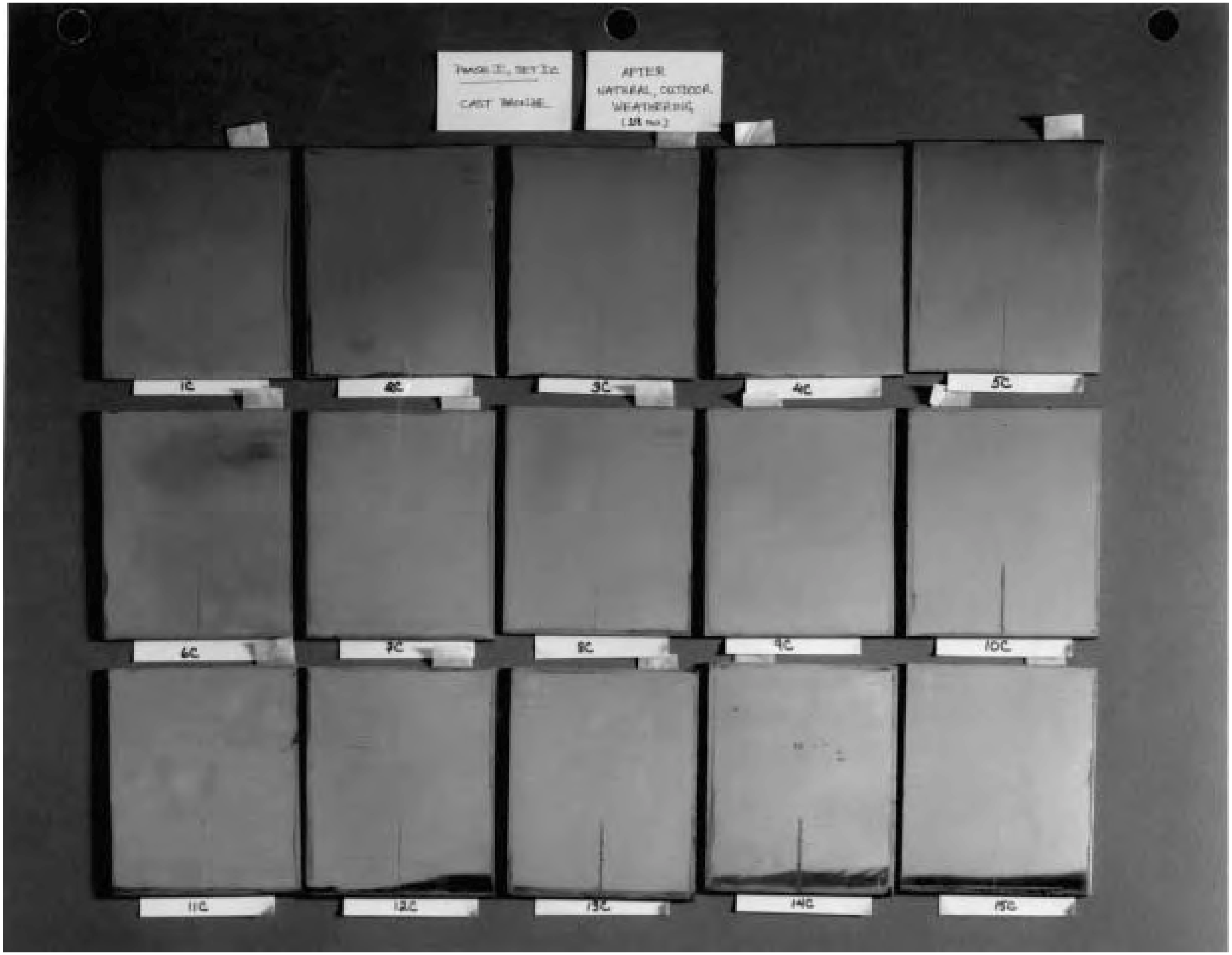
PHASE II, SET IC
CAST BRONZE
AFTER
NATURAL, OUTDOOR
WEATHERING
(18 mo.)
1C
2C
3C
4C
5C
6C
7C
8C
9C
10C
11C
12C
13C
14C
15C

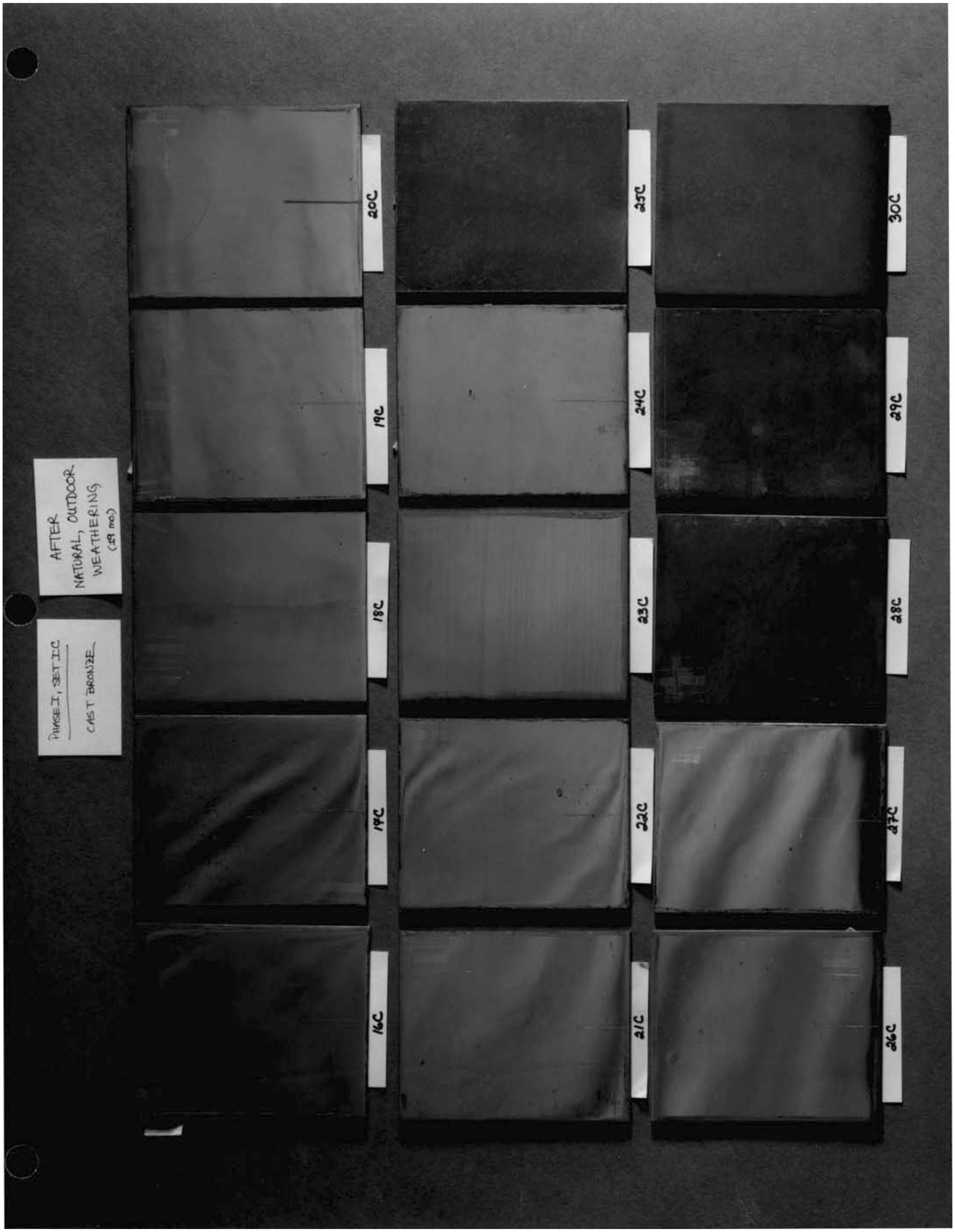
PHASE I, SET IC
CAST BRONZE
AFTER
NATURAL, OUTDOOR
WEATHERING
(19 mo.)
16C
17C
18C
19C
20C
21C
22C
23C
24C
25C
26C
27C
28C
29C
30C

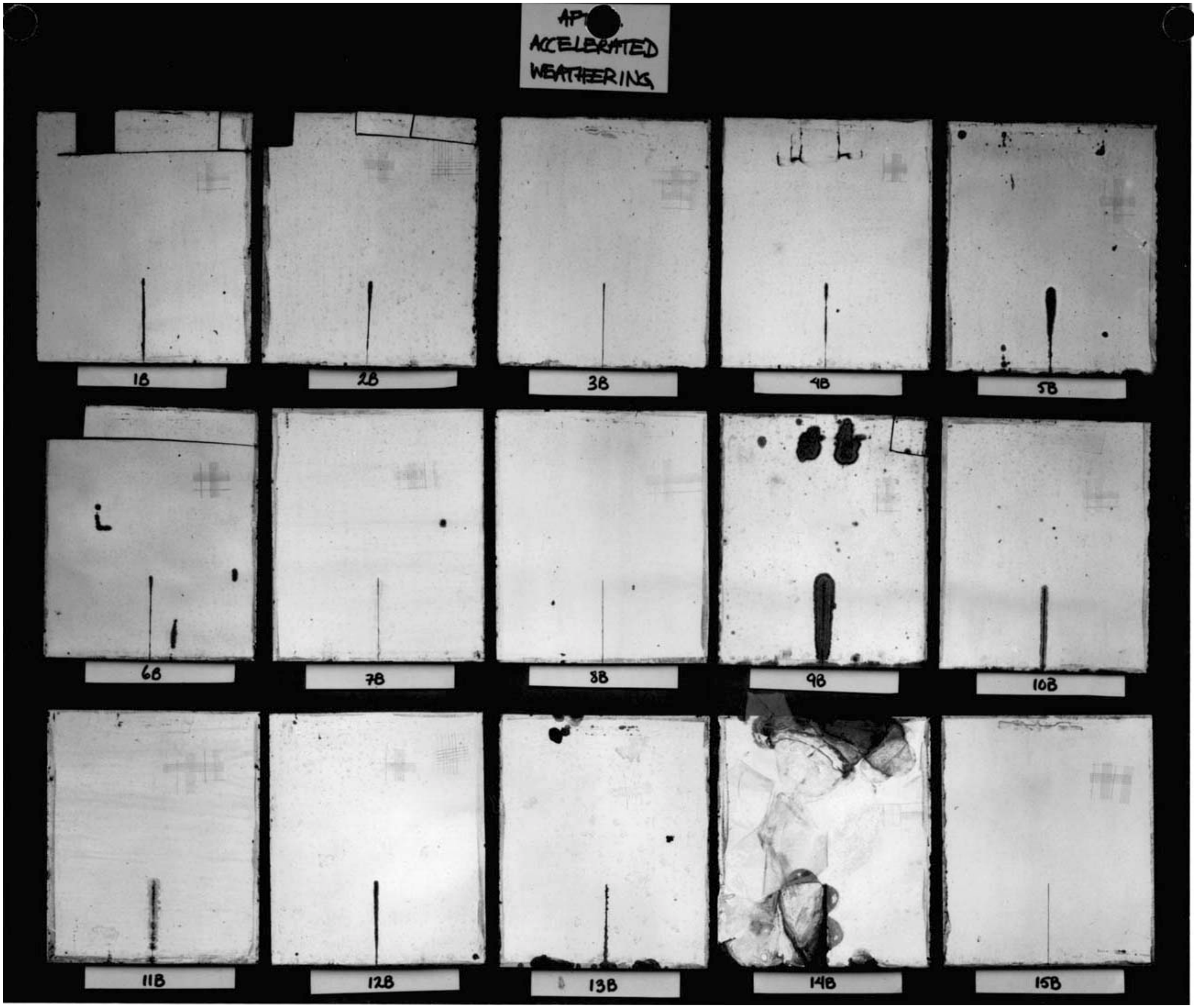
AP
ACCELERATED
WEATHERING
1B
2B
3B
4B
5B
6B
7B
8B
9B
10B
11B
12B
13B
14B
15B


APT
ACCELERATED
WEATHERING
16B
19B
18B
19B
20B
21B
22B
23B
24B
25B
26B
27B
28B
29B
30B

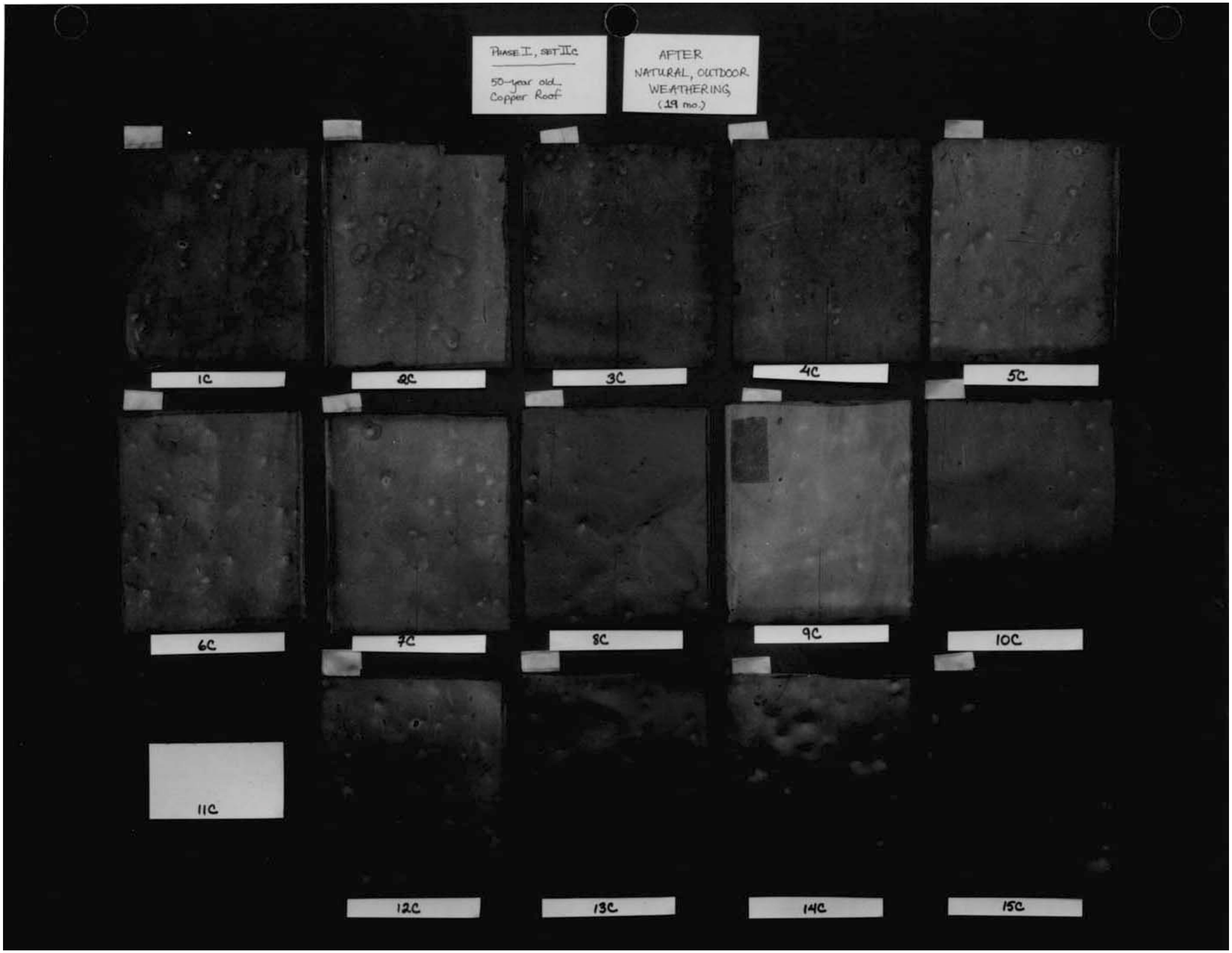
PHASE I, SET IIc
50-year old
Copper Roof
AFTER
NATURAL, OUTDOOR
WEATHERING
(19 mo.)
1C
2C
3C
4C
5C
6C
7C
8C
9C
10C
11C
12C
13C
14C
15C

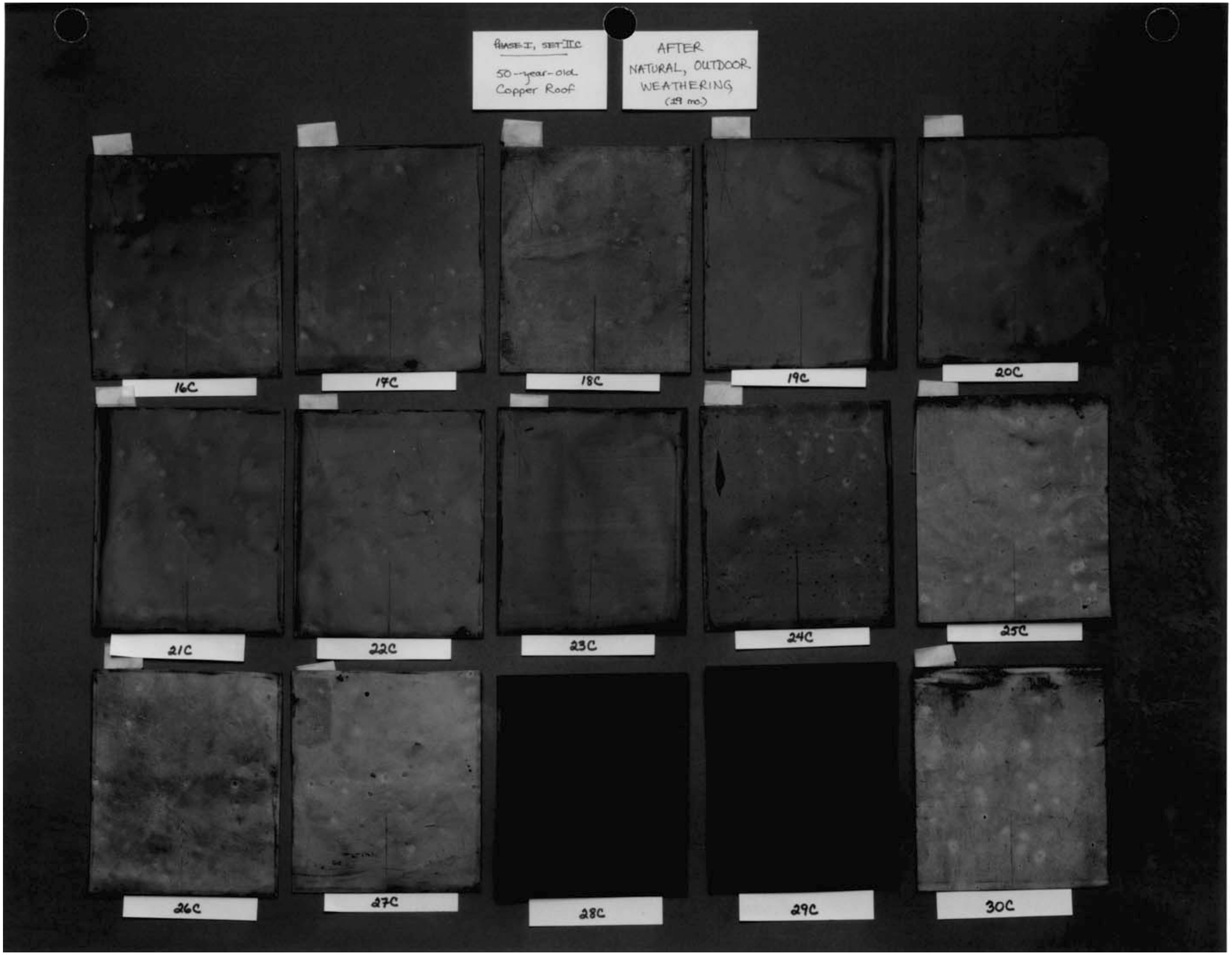
PHASE I, SET IIC
50-year-old Copper Roof
AFTER NATURAL, OUTDOOR WEATHERING (19 mo.)
16C
17C
18C
19C
20C
21C
22C
23C
24C
25C
26C
27C
28C
29C
30C


AFTE
ACCELERATED
WEATHERING
1B
2B
3B
4B
5B
6B
7B
8B
9B
10B
11B
12B
13B
14B
15B


AFTE
ACCELERATED
WEATHERING
16B
17B
18B
19B
20B
21B
22B
23B
24B
25B
26B
27B
28B
29B
30B

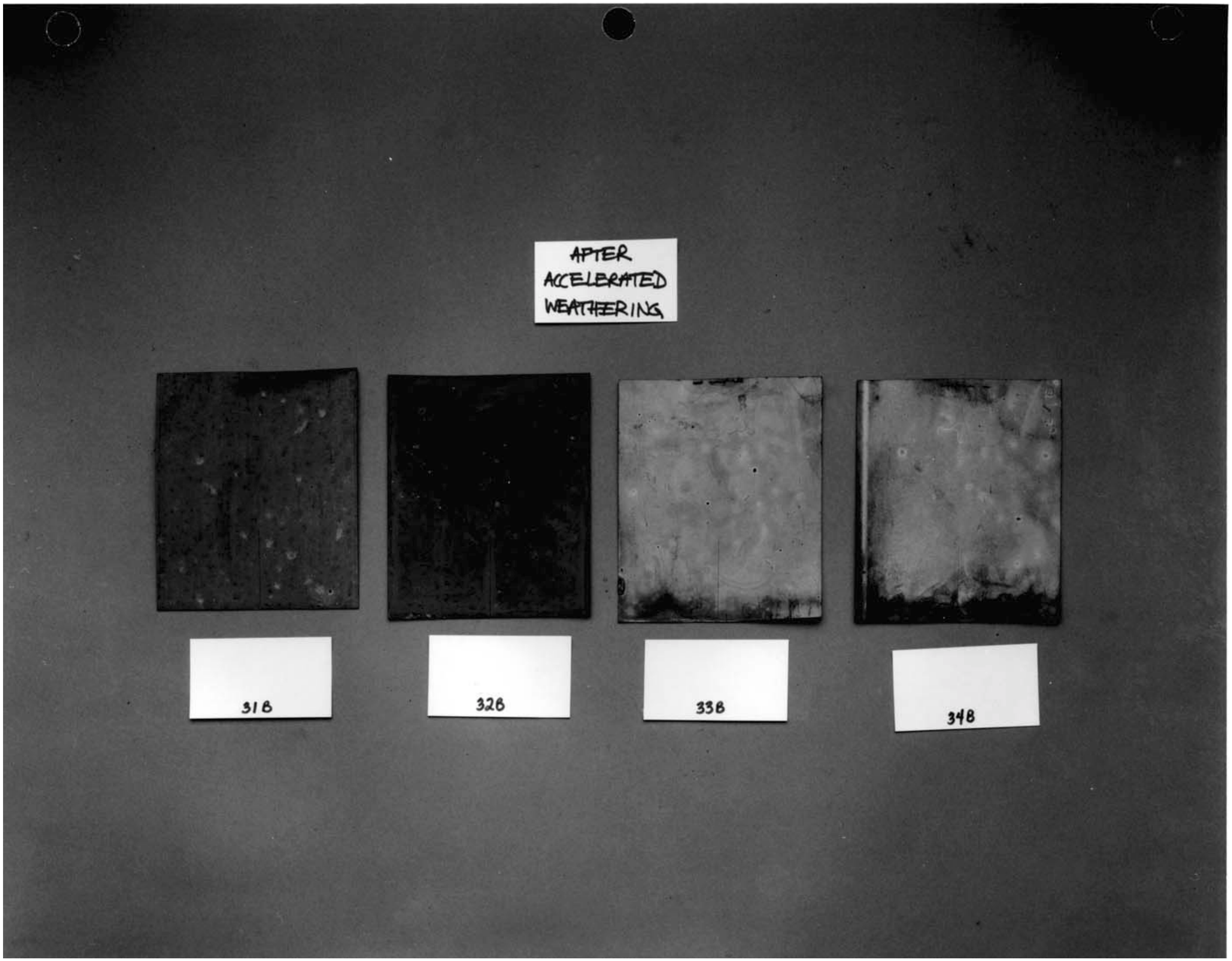
AFTER
ACCELERATED
WEATHERING
31B
32B
33B
34B


BEFORE WEATHERING
Set I. CAST BRONZE
1. Incralac + wax
2. BTA pt. + wax
3. NK 11565 + NK 9778 + wax
4. BASF 923-85 + wax
5. NK 11560 + wax
6. uncoated controls
A
Ba
Bb
Bc
C
Silane
Incralac

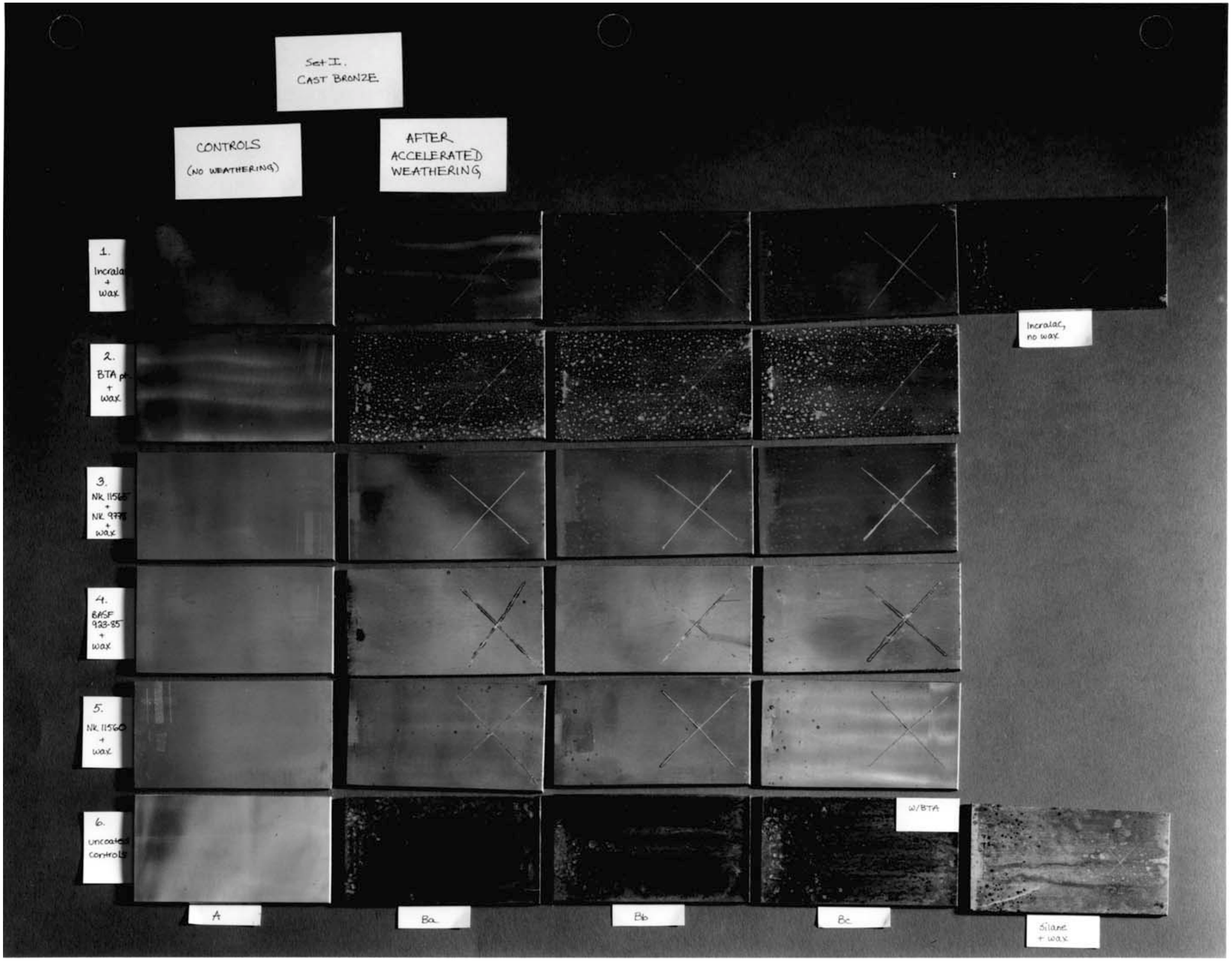
Set I.
CAST BRONZE
CONTROLS
(NO WEATHERING)
AFTER
ACCELERATED
WEATHERING
1.
Incrala
+
wax
Incralac,
no wax
2.
BTA p
+
wax
3.
NK 11565
+
NK 9778
+
wax
4.
BASF
923-85
+
wax
5.
NK 11560
+
wax
6.
Uncoated
Controls
w/BTA
Silane
+ wax
A
Ba
Bb
Bc


BEFORE WEATHERING
Set II Patinated, cast Bronze
1. Incralac + wax
2. BTA pt. + wax
3. NK 11565 + NK 9778 + wax
4. BASF 923-85 + wax
5. NK 11560 + wax
6. uncoated controls
A
Ba
Bb
Bc
C

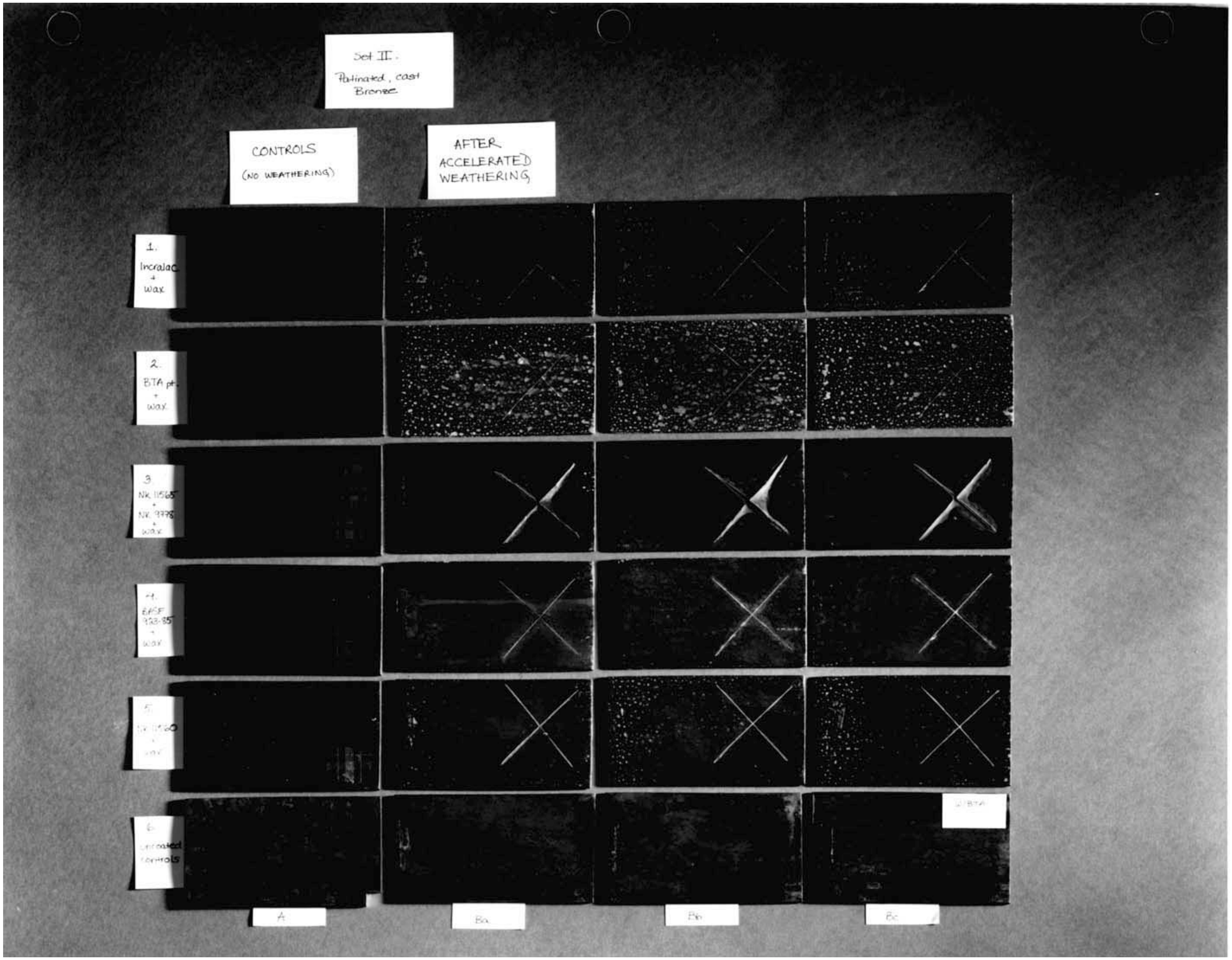
Set II.
Patinated, cast Bronze
CONTROLS (NO WEATHERING)
AFTER ACCELERATED WEATHERING
1. Incralac + wax
2. BTA pt. + wax
3. NK 11565 + NK 9778 + wax
4. BASF 923-85 + wax
5. NK 11560 + wax
6. Uncoated controls
w/BTA
A
Ba
Bb
Bc

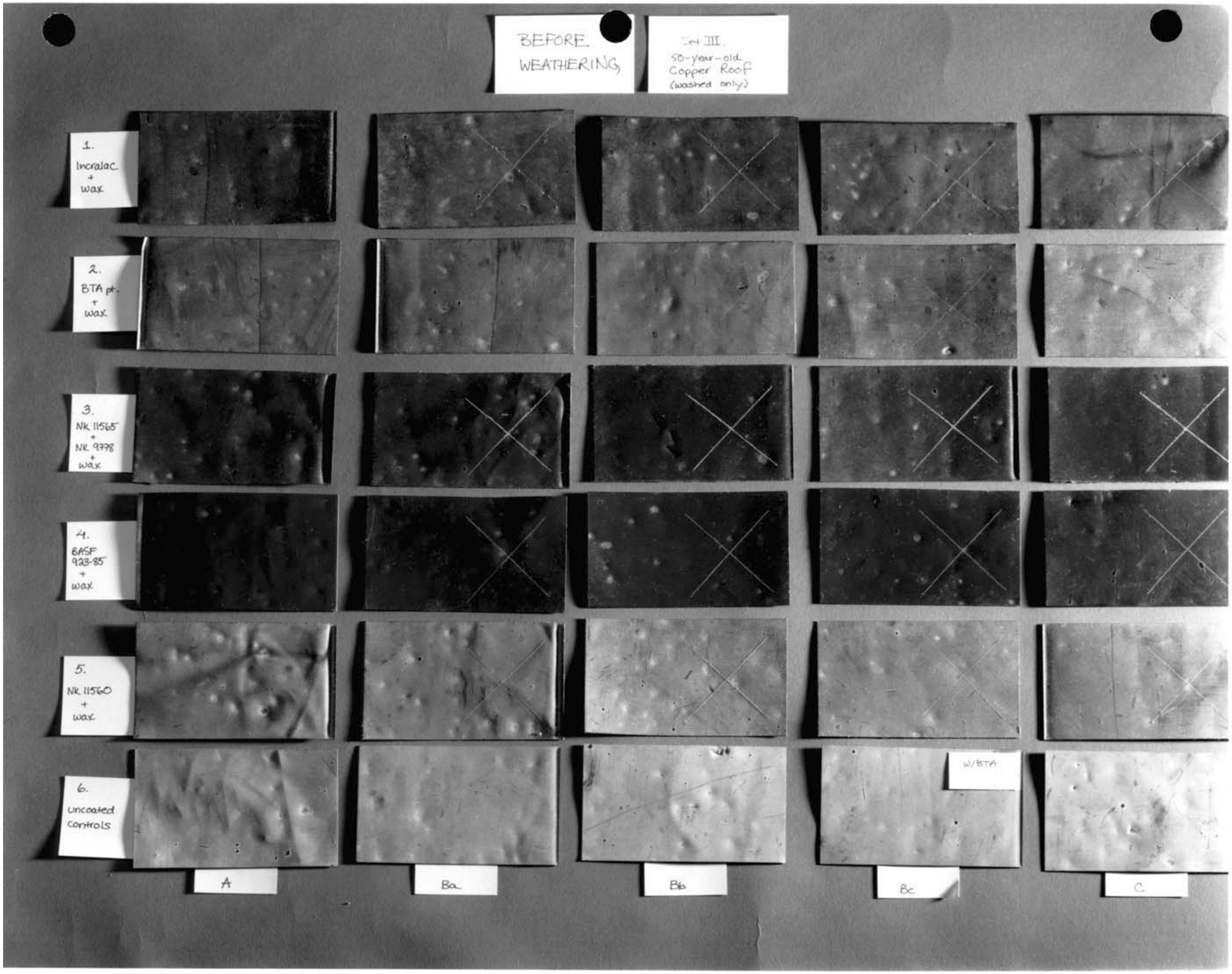
BEFORE WEATHERING,
Set III, 50-year-old Copper Roof (washed only)
1. Incralac + wax
2. BTA pt. + wax
3. Nk 11565 + NK 9778 + wax
4. BASF 923-85 + wax
5. NK 11560 + wax
6. Uncoated Controls
W/BTA
A
Ba
Bb
Bc
C

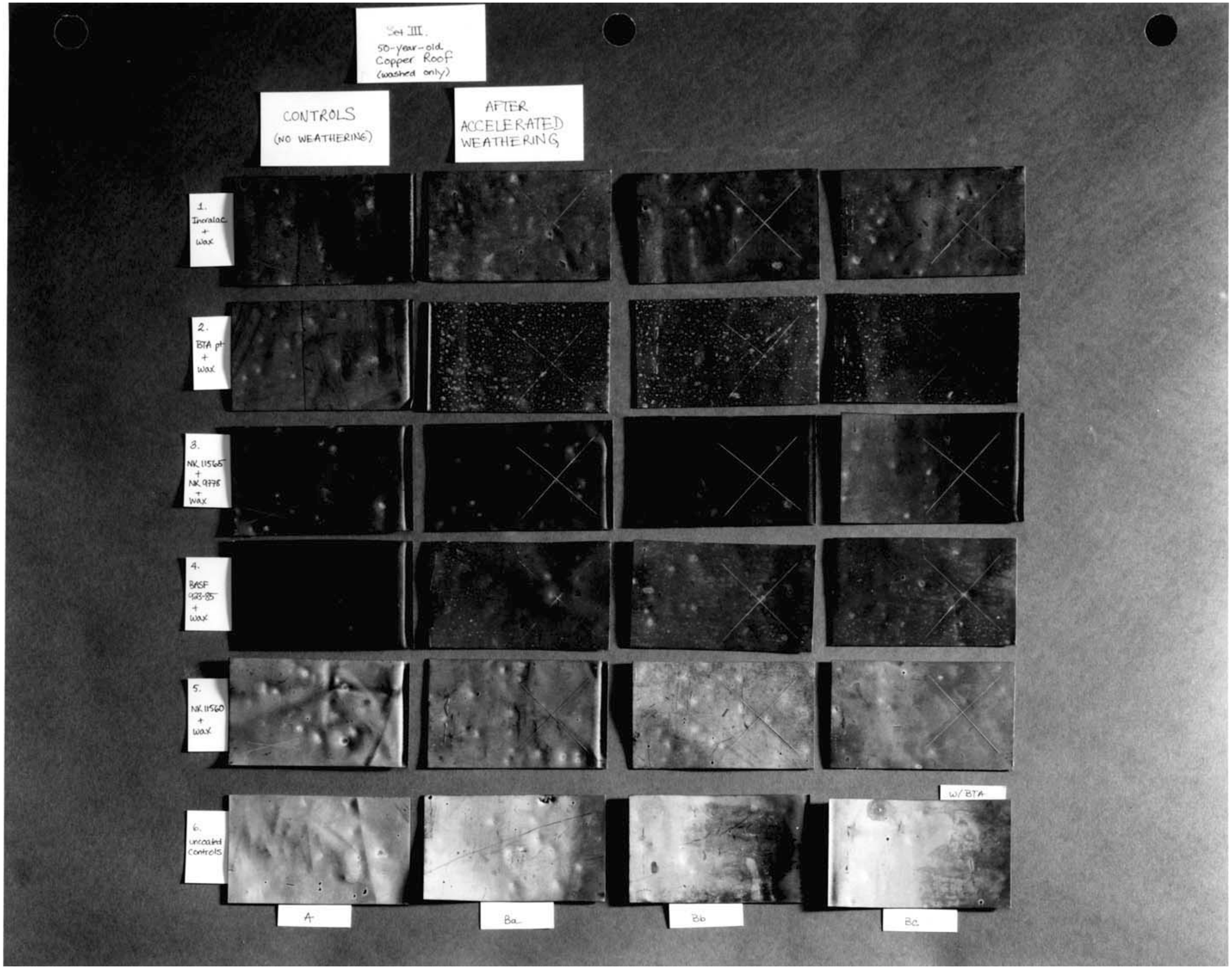
Set III.
50-year-old Copper Roof (washed only)
CONTROLS (NO WEATHERING)
AFTER ACCELERATED WEATHERING
1. Incralac + wax
2. BTA pt + wax
3. NK 11565 + NK 9778 + wax
4. BASF 923-85 + wax
5. NK 11560 + wax
6. uncoated Controls
W/BTA
A
Ba
Bb
Bc

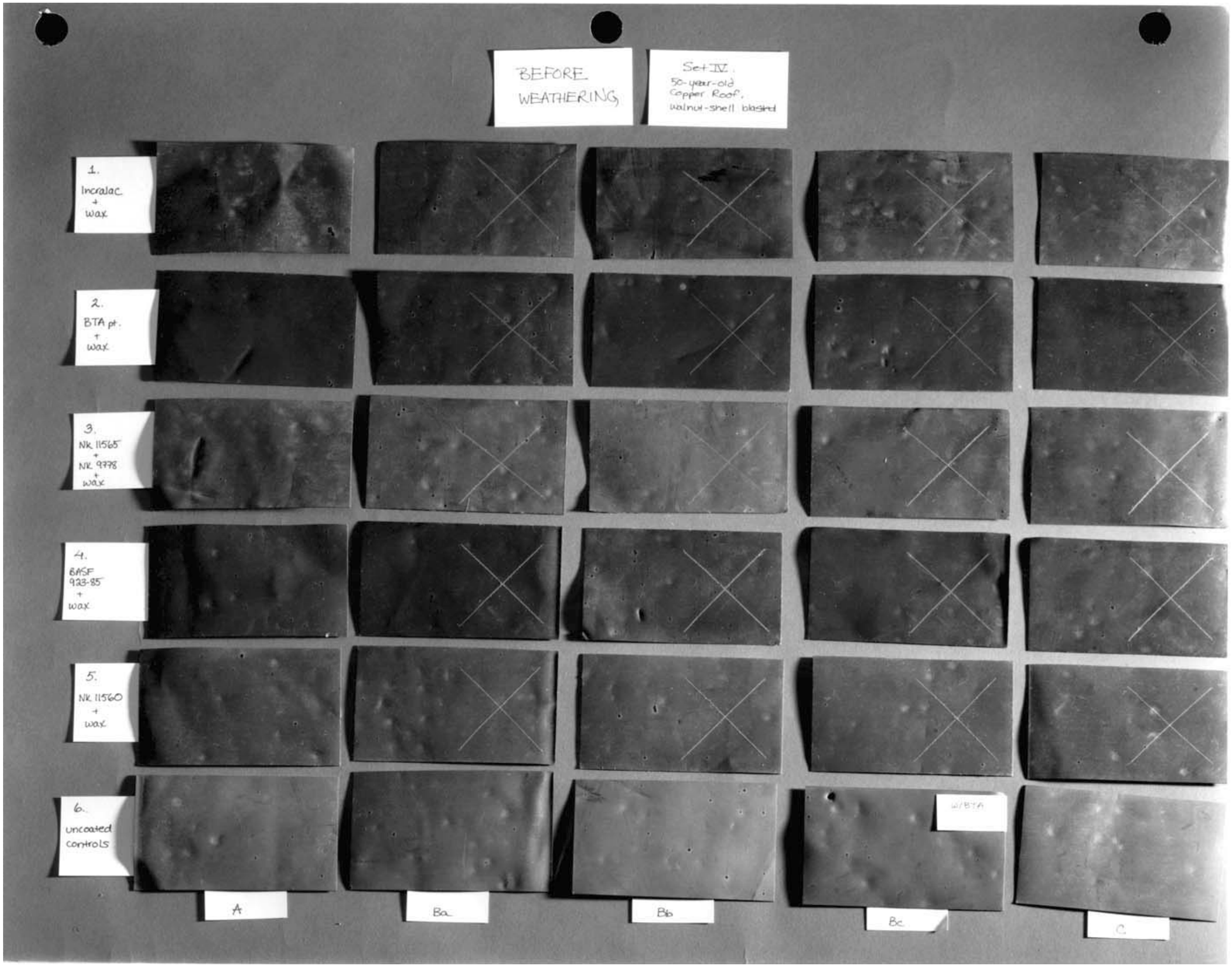
BEFORE WEATHERING
Set IV.
50-year-old
Copper Roof,
walnut-shell blasted
1. Incralac + wax
2. BTA pt. + wax
3. NK 11565 + NK 9778 + wax
4. BASF 923-85 + wax
5. NK 11560 + wax
6. Uncoated controls
w/BTA
A
Ba
Bb
Bc
C

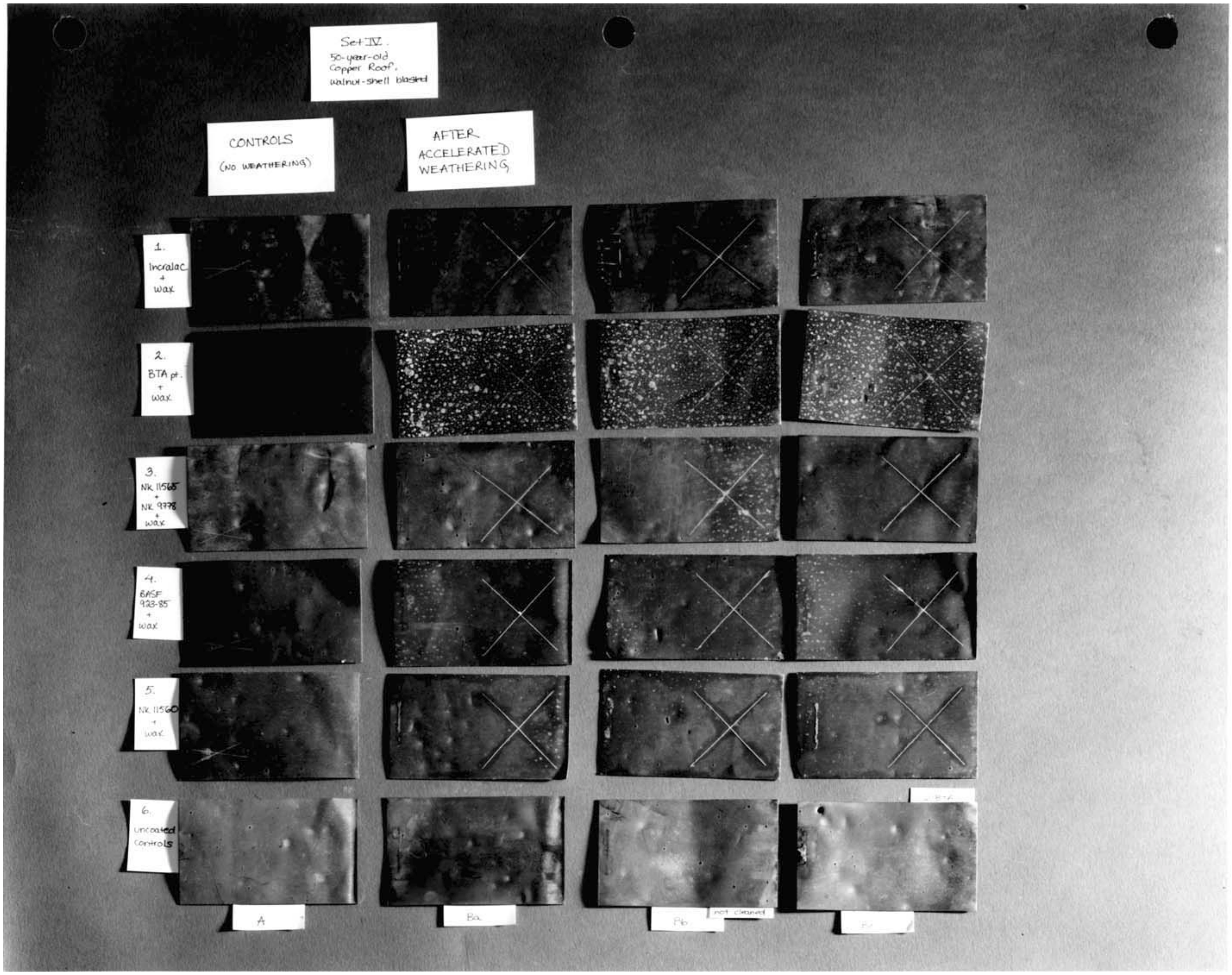
Set IV.
50-year-old
Copper Roof,
walnut-shell blasted
CONTROLS
(NO WEATHERING)
AFTER
ACCELERATED
WEATHERING
1. Incralac + wax
2. BTA pt. + wax
3. NK 11565 + NK 9778 + wax
4. BASF 923-85 + wax
5. NK 11560 + wax
6. Uncoated controls
A
Ba
Bb
not cleaned
Bc